TECHNICAL UNIVERSITY OF LIBEREC
Faculty of Textile Engineering

Study and analysis of a Polycaprolactone polymeric solution to produce a nanofibrous coating for medical stitching threads via electrospinning

Master Thesis

Study programme:	N3106 Textile Engineering
Study branch:	Nonwoven and Nanomaterials
Author:	**Juan Pablo Pérez Aguilera**
Thesis Supervisors:	prof. RNDr. David Lukáš, CSc. Department of Chemistry

Liberec 2021

TECHNICAL UNIVERSITY OF LIBEREC
Faculty of Textile Engineering

Master Thesis Assignment Form

Study and analysis of a Polycaprolactone polymeric solution to produce a nanofibrous coating for medical stitching threads via electrospinning

Name and surname: **Juan Pablo Pérez Aguilera**
Identification number: T18000017
Study programme: N3106 Textile Engineering
Study branch: Nonwoven and Nanomaterials
Assigning department: Department of Nonwovens and Nanofibrous materials
Academic year: **2019/2020**

Rules for Elaboration:

1. Literature review focused on properties of gels, sol-gel transitions, solubility of polymeric solutions and AC electrospinning.
2. Determination of parameters to use in samples for experiments.
3. Measurement of stability of samples from preliminary experimentation and preparation of following experiments.
4. Study of characteristics and spinnability of stable samples. Characterization and measurement of properties of resulting nanofibrous coating.
5. Results discussions, drawing of conclusions and following steps.

Scope of Graphic Work:
Scope of Report: 40-60
Thesis Form: printed/electronic
Thesis Language: English

List of Specialised Literature:

1. F. Tanaka and A. Matsuyama, "Theory of Solvation-Induced Reentrant Phase Separation in Polymer Solutions," Physical Review Letters, pp. 70-75, 1990.
2. C. Bordes, V. Fréville, E. Ruffin, P. Marote, J. Gauvarit, S. Briancon and P. Lantéri, Pharmaceutical Nanotechnology, pp. 236-243, 2010.
3. C. Luo, E. Stride and M. Edirisinghe, "Mapping the Influence of Solubility and Dielectric Constant on Electrospinning Polycaprolactone Solutions," Macromolecules, pp. 69-80, 2012.
4. H. Wen and H. Zhen-Ming, "Development of Functional Sutures through Electrospinning," Tongji University, Shanghai.

Thesis Supervisors: prof. RNDr. David Lukáš, CSc.
Department of Chemistry

Date of Thesis Assignment: January 6, 2020
Date of Thesis Submission: January 10, 2021

L.S.

Ing. Jana Drašarová, Ph.D.
Dean

Ing. Jiří Chvojka, Ph.D.
Head of Department

Liberec January 6, 2020

Declaration

I hereby certify, I, myself, have written my master thesis as an original and primary work using the literature listed below and consulting it with my thesis supervisor and my thesis counsellor.

I acknowledge that my bachelor master thesis is fully governed by Act No. 121/2000 Coll., the Copyright Act, in particular Article 60 – School Work.

I acknowledge that the Technical University of Liberec does not infringe my copyrights by using my master thesis for internal purposes of the Technical University of Liberec.

I am aware of my obligation to inform the Technical University of Liberec on having used or granted license to use the results of my master thesis; in such a case the Technical University of Liberec may require reimbursement of the costs incurred for creating the result up to their actual amount.

At the same time, I honestly declare that the text of the printed version of my master thesis is identical with the text of the electronic version uploaded into the IS/STAG.

I acknowledge that the Technical University of Liberec will make my master thesis public in accordance with paragraph 47b of Act No. 111/1998 Coll., on Higher Education Institutions and on Amendment to Other Acts (the Higher Education Act), as amended.

I am aware of the consequences which may under the Higher Education Act result from a breach of this declaration.

January 8, 2021 Juan Pablo Pérez Aguilera

ABSTRACT

Stability of polymeric solutions is a highly important characteristic for the production process of nanofibers that will be used in filtration, medicine, biotechnology and electronics among other applications. Without a stable polymeric solution there will be phase separation [1]. This generates problems because the polymer will collapse on itself and form globules, which makes electrospinning impossible [2]. The stability of these solutions depends on atmospheric properties (temperature, atmospheric pressure, humidity, etc.), osmotic pressure and interaction parameters of the polymer among other properties [3]. Stability at defined conditions will be different for each polymeric solution. This diploma project will focus on a solution of Polycaprolactone on Acetic acid, Formic acid and acetone, which will be used in electrospinning to produce a nanofiber coating layer used on a polylactic acid filament; thus, creating an improved and highly biocompatible stitching thread [4]. The challenge is that this specific polymeric solution shows phase separation at atmospheric conditions. On the other hand, under 3ºC this solution forms a thermo-reversible gel which is stable and can be used in electrospinning, this effect is observable in the samples studied by professor David Lukáš in the TUL laboratories. Therefore, the focus of this diploma project will be studying and understanding the stability of this solution in order to correctly quantify the phase transition temperature and allow for stable storage and posterior electrospinning to ensure the quality of the nanofibrous coating.

KEYWORDS

Polycaprolactone, polymer-solvent system, sol-gel phase transition, phase transition temperature, electrospinning, nanofibers, sutures, medical textiles.

OBJECTIVE

To understand and describe the conditions required for the dissolution of polycaprolactone (PCL) in acetic acid (AA), formic acid (FA) and acetone (Ac) that will allow stable storage for posterior electrospinning and production of a functional nanofibrous coating. As well as the investigation for a deeper understanding of the sol-gel thermoreversible phase transition of this polymer-solvent system.

ABSTRAKT

Stabilita polymerních roztoků je velmi důležitou charakteristikou pro proces výroby nanovláken, která se budou mimo jiné používat ve filtraci, medicíně, biotechnologii a elektronice. Bez stabilního polymerního roztoku dojde k fázové separaci [1]. To vytváří problémy, protože polymer se sám zhroutí a vytvoří kuličky, což znemožňuje elektrostatické zvlákňování [2]. Stabilita těchto roztoků závisí mimo jiné na atmosférických vlastnostech (teplota, atmosférický tlak, vlhkost atd.), osmotickém tlaku a parametrech interakce polymeru [3]. Stabilita za definovaných podmínek bude pro každý polymerní roztok odlišná. Tato diplomová práce se zaměří na roztok polykaprolaktonu na kyselině octové, kyselině mravenčí a acetonu, který bude použit při elektrostatickém zvlákňování k výrobě nanovlákenné potahové vrstvy používané na vláknu polymléčné kyseliny; tedy vytvoření vylepšené a vysoce biokompatibilní šicí nitě [4]. Úkolem je, že tento specifický polymerní roztok vykazuje za atmosférických podmínek fázovou separaci. Na druhé straně, při teplotě nižší než 3°C toto řešení tvoří termo-reverzibilní gel, který je stabilní a lze jej použít při elektrostatickém zvlákňování, tento účinek je pozorovatelný u vzorků studovaných profesorem Davidem Lukášem v laboratořích TUL. Cílem diplomové práce bude proto studium a porozumění stabilitě tohoto řešení za účelem správné kvantifikace teploty fázového přechodu a umožnění stabilního skladování a pozdějšího elektrostatického zvlákňování, aby byla zajištěna kvalita nanovlákenného povlaku.

KLÍČOVÁ SLOVA

Polykaprolakton, systém polymer-rozpouštědlo, fázový přechod sol-gel, teplota fázového přechodu, elektrostatické zvlákňování, nanovlákna, stehy, lékařské textilie.

CÍL

Pochopit a popsat podmínky potřebné pro rozpuštění polykaprolaktonu (PCL) v kyselině octové (AA), kyselině mravenčí (FA) a acetonu (Ac), které umožní stabilní skladování pro pozdější elektrostatické zvlákňování a výrobu funkčního nanovlákenného povlaku, stejně jako výzkum pro hlubší pochopení termoreverzibilního fázového přechodu sol-gel tohoto systému polymer-rozpouštědlo.

AKNOWLEDGEMENTS

I would like to thank the following people who have helped me undertake this diploma project.

First my supervisor, Prof. David Lukáš for his guidance, teachings and encouraging words during my time as his student. I feel extremely lucky for having the opportunity to work with a supervisor who irradiates inspiring passion for research and the pursuit of knowledge.

Manikandan Sivan and Divyabharathi Madheswaran for helping me learn the ropes in the laboratory and providing guidance and advice regarding the project and the academical life in general.

Stepan Kunc for his participation on the design and set-up of the laser-thermometer experimental apparatus used in the final tests of this diploma project. His knowledge of the equipment and software were invaluable in the creation of this apparatus.

Eva Kuželová Košťáková for her contribution with the collection of microscope images of the system using a specialized Leica DVM6 digital microscope. This allowed to better understand the system studied in the project.

Hana Musilová for her extreme patience, guidance and encouraging words during my whole student life at TUL. She was always there to lend a hand with comforting smile.

The whole Textile Faculty at TUL for their teachings and generating a space where I could develop in a professional field of my interest.

To my parents, Raúl Antonio Pérez Bonna and Aurora Aguilera Huerfano. Who have been the biggest inspiration in my life to always become a better person in every aspect, I will dedicate a few words in Spanish for them. Gracias por ser siempre una fuente inagotable de apoyo, sabiduría, amor e inspiración. Todos mis logros son gracias a ustedes, me siento afortunado y orgulloso de que sean mis padres. Los amo.

To Sena Toktaş, for her love and support during the good times and the harsh times. And specially for always making me smile and inspiring me to be the best version of myself and give my best to every challenge. Thank you.

And to all my friends and family that were always there for me making heavy situations lighter and shinning their lights on my path.

TABLE OF CONTENTS

LIST OF SYMBOLS

F: $Free\ energy\ of\ the\ system$

U: $Internal\ energy\ of\ the\ system$

T: $Transition\ temperature$

T_0: $Initial\ temperature\ of\ the\ system$

S: $Thermodynamic\ entropy\ of\ the\ system$

σ: $Statistical\ entropy\ of\ the\ system$

k_b: $Boltzmann\ constant$

g: $Number\ of\ possible\ configurations\ of\ the\ binary\ misxture\ on\ the\ lattice$

n: $Total\ number\ of\ nodes\ in\ the\ lattice$

n_i: $Number\ of\ nodes\ in\ the\ lattice\ occupied\ by\ substance\ i$

ϕ_i: $Fraction\ of\ the\ latice\ occupied\ by\ substance\ i$

N_i: $Polymerization\ degree\ of\ the\ substance\ i$

χ: $Interaction\ parameter$

ε_{pp}: $Interaction\ energy\ between\ non-covalent\ bonded\ polymer\ molecules$

ε_{ss}: $Interaction\ energy\ between\ solvent\ molecules$

ε_{ps}: $Interaction\ energy\ between\ polymer\ and\ solvent\ molecules$

z: $Coordination\ number$

G: *Entropic term related to the number of configurations of the polymeric chains pre and post mixing*

1. INTRODUCTION

Technical textiles made their way into the medical field, creating a mixed field called medical textiles. This is a broad area of study in which textile materials have seen an enormous surge in application and usage in the present era due to their versatility, simplicity of use and easy manufacturing process. Currently, there is a wide variety of medical textiles that cover a plethora of applications. Medical textiles are classified into four different groups; Healthcare and hygiene, extracorporeal devices, non-implantable materials and implantable materials [1]. As a general rule, the materials used for these applications are required to have the following relevant properties. Non-toxic, sterilization capabilities, good mechanical properties, non-allergic response, biodegradability and biocompatibility. With the last two properties being of vital importance for the development of new and innovative implantable materials.

Inside healthcare and hygiene there are textile products such as medical scrubs, facemasks, nonwoven disinfectant wipes and other general protective equipment usually found in hospitals or being worn by medical staff. These products are usually disposable, which means that they have low production costs and are highly available. Among the most used fibers for these applications are common ones such as polyester, polypropylene, cotton, etc. The kind of fabric found in these products can be either woven or non-woven. In the category of extracorporeal devices, the textile materials used require a more refined preparation for use due to the fact that these devices are implemented in order to function as support for vital organs. For example, an artificial liver requires hollowed viscose fibers. While an artificial kidney uses hollow polyester fibers and a mechanical lung requires a hollow silicone membrane and hollow polypropylene fibers. These materials are required to work with as little maintenance as possible due to the importance of their function [2].

The other two categories include products used for wound and trauma treatment. The non-implantable materials are used for external support and may or may not be in direct contact with the affected tissue. In this category there is a wide variety of both synthetic and natural fibers being used and these fibers are combined to form a wide variety of woven and non-woven fabrics. Thus, the production costs and durability of these products depends mainly on the type of wound/trauma they will be treating, as well as the intensity of the required treatment. Some examples of these medical devices are compression bandages, plasters, orthopedic supports and gauze dressings, among others [1].

On the other hand, implantable materials are medical devices that are implemented in high impact repairs required on the body. These can be either tissue regeneration, wound closure or surgical tissue replacement. In the case of tissue regeneration and tissue replacement, there are various new techniques and technologies that allow for striking a good balance between desired mechanical properties, biocompatibility and biodegradability. These devices are required to stay in the body for prolonged periods of time. Depending on the type of treatment they can even be implanted for years before requiring maintenance or replacement. For example, vascular grafts are required to stay in the body for long periods of time with vital functions, while synthetic extracellular matrices (scaffolds) are required to stay in the body

without rejection only during the healing period, after that they need to be absorbed by the system [3]. On the case of wound closure, the most widely used method is with sutures. It is a true and tested method that has been in the medical field since as early as the old Egyptian empire. In current times these devices are evolving towards using surface modification techniques to improve biocompatibility and biodegradability; because, just like the implantable scaffolds, sutures should stay in the tissue as long as the healing process requires them. After that the desired result is for them to be absorbed by the system [4].

In this diploma project the focus will be on a system designed to aid the sutures in wound closure. By introducing electrospun polycaprolactone (PCL) nanofibers on the surface of a medical device, the biocompatibility of said device is improved [5]. Electrospinning is a technology that has been very relevant in the Technical University of Liberec, therefore the spinnability of these nanofibers has been of great interest for the institution. The base system of interest consists of 10%w/vol PCL dissolved in a solvent system of acetic acid (AA), formic acid (FA) and acetone (At) in a mixing volumetric ratio of 1:1:1. This system was observed, by the research group directed by D. Lukas and M. Sivan from TUL, to stop the hydrolytic degradation of the PCL in the solvent system by being introduced in a freezer and forming a thermoreversible gel. As a result, this project was created in order to understand and study the behavior of the PCL solution used in the electrospinning. This knowledge will be used to ensure the safe storage of the solution in order for it to be spinnable and stable after extended periods of time.

2. STATE OF THE ART

Sutures are a thread-like textile medical devices that can either be monofilaments or multifilament in twisted or braided form. As all textiles, sutures can be either natural or synthetic depending on the desired mechanical properties [6]. Also classified as a bio textile, sutures always perform in contact with cells in a biological medium. Their efficiency depends on their interactions with the tissue, this is assessed by evaluating the biostability and biocompatibility of the material [4]. They play a crucial role in medicine, especially in surgical interventions. The suture is used to close any kind of wound where tissue needs to be held in position in order for it to heal correctly [7]. It is of high importance to select the correct material and treatment for the thread that will be applied to a specific injury, due to the specific mechanical properties requirements each tissue has. If the suture fails, there will be severe consequences which include heavy hemorrhage, infection of the affected tissue or incorrect healing of connective tissue in sensitive areas [8].

Surgical sutures can be classified depending on their origin, structure or biodegradability. As shown in Fig 2.1.

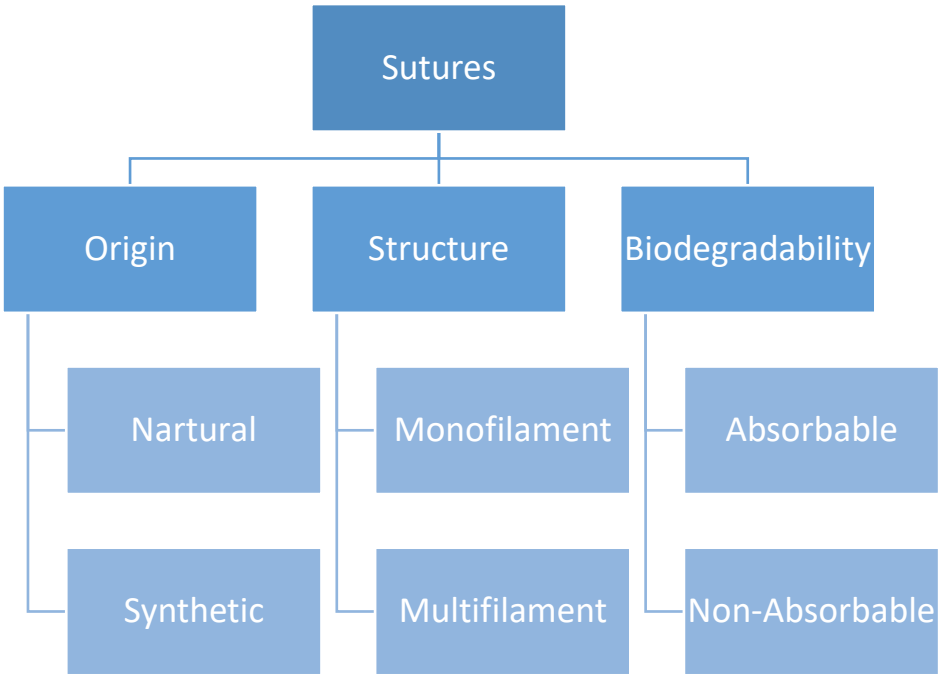

Figure 2.1. *Classification of surgical sutures [9].*

The most important characteristic for the applications of sutures in the field of medicine is the biodegradability factor. Non-absorbable sutures remain in the human body for more than 60 days after implantation without any significant loss of mechanical properties. On the other hand, absorbable sutures have a continuous loss of mechanical properties during the first 60 days after implantation in the tissue. Before this period is over, enzymatic activity and

hydrolysis processes degrade the polymer into non-cytotoxic organic molecules that are absorbed by the human body [10].

This classification is enough to cover most, if not all the traditional yarns used for the fabrication of sutures. But in the case of newer and innovative composite yarns, such as the case of the composite yarn with a PCL nanofibrous coating, this classification system is not enough. This composite yarn was tested by another investigation group from TUL before using a core of Polylactic acid (PLA) with a smooth surface where the nanofibers where added by AC electrospinning. So, this would classify as a synthetic and multifilament yarn, but in terms of biocompatibility it is both absorbable (from the PCL nanofibers) and non-absorbable (from the PLA core).

Table 2.1. *Advantages and disadvantages of sutures based on the classification seen in Fig. 2.1* [11].

Classification		**Advantages**	**Disadvantages**
Origin	Natural	- High tensile strength retention during absorption - Fast absorption	- High chance of causing an inflammatory reaction - Low initial tensile strength
	Synthetic	- Low chance to cause an inflammatory response - Better mechanical properties than natural sutures	- Susceptible to hydrolysis - Slower absorption, could require medical removal
Structure	Monofilament	- Low resistance from the tissue - Low chance of infection due to smooth structure	- Poor knot security - Weak spots are easily created by mishandling
	Multifilament	- High knot security - Low risk of creating weak spots - Improved mechanical properties	- High resistance from the tissue - High risk of harboring organisms resulting in infection - Antimicrobial agent required
Biodegradability	Absorbable	- No removal required	- Loss of mechanical properties over time
	Non-Absorbable	- Provide long term support for the tissue - Good retention of mechanical properties	- Foreign body left in the tissue - Removal required to finish the treatment

As observed in table 2.1, the classification of sutures can indicate the general characteristics to be expected from a specific suture with a given origin, structure and biodegradability. Thus, the requirements to treat each specific wound in different kind of tissue can be easily met. This, combined with an adequate needle and the correct stitching pattern make the suture an invaluable tool for the closing and correct healing of wounds.

Taking the information from table 2.1 into account, the expected characteristics of a suture consisting of a PLA core with a PCL nanofibrous coating are the following. From the synthetic nature of the PLA core a slow absorption time is expected, this is counteracted by the absorbable character the PCL nanofibers bring to the table. In turn, the PCL nanofibers alone would show a high loss of mechanical properties over time, which is solved thanks to the inclusion of the PLA core and the multifilament nature of the composite yarn.

2.1. Surface modifications in sutures

The latest advances in the field of surgical sutures comes in the form of surface modifications. This gives the opportunity of modifying and designing a wide range of properties that will have significant effects on the performance of the suture. Modifications can be made to characteristics such as cross section shape, surface roughness and addition of antimicrobial agents among others [12]. Various technologies have been developed on this field in order to obtain innovative results.

2.1.1. Plasma treatment

Surface modifications often include the linking of additional structures to the external layer of the material; thus, obtaining different characteristics without affecting the bulk properties of the suture. Plasma treatment is used in order to prepare the surface to improve the bonding between the surface and the added substance. This is done by exposing a gas to an electric potential difference that will transform it into a cloud of molecular fragments (anions, cations, free electron, free radicals, etc.) that will collide with the surface of the suture and open up bonds, clean impurities to generate hydrophobicity or hydrophilicity and create new functional groups [13]. The value of plasma treatment comes with its versatility and the eco-friendliness of the process, due to it being a dry process that doesn't generate waste. A recent research carried out in the Technical University of Liberec by Sivan et al [14], shows the increase of the surface wettability of PCL nanofibrous mats by applying argon and nitrogen via plasma treatment. The treated samples did not suffer any alterations to their morphological properties.

2.1.2. Particle dispersion

To achieve additional properties such as drug delivery over a specific timeframe, antimicrobial effect, improved mechanical properties, improved absorption and adsorption properties among others. Non-miscible metallic particles (silver) or other natural/synthetic polymeric particles are dispersed in the polymeric solution before this one is drawn into fibers

to form the suture. In the case of natural sutures, inert and insoluble polymeric microparticles are used to impregnate the bulk material and ensure it penetrates through the fibers; afterwards, the suture is centrifuged to eliminate any excess moisture [15]. In most cases, the dispersed particles are held in place due to electrostatic charge difference with the surface or the polymer. On the other hand, friction and Van der Waals forces also come into play in retaining the particles. This technique offers great possibilities in the form of more reliable supportive properties, such as the treatment of inflammation with ibuprofen (nonsteroidal anti-inflammatory agent) delivering sutures [16].

2.1.3. Coating with biocompatible materials

Coating sutures is common practice, especially in the case of multifilament surgical sutures. The coating is applied not only to help with identification, but also to counter act the most common disadvantages present in this kind of sutures. This technique reduces tissue drag, increases knot security and eases the handling in practice. Biocompatible materials are used for the coating of sutures and they can either be water-soluble or insoluble. Water-soluble coatings are dissolved rapidly after the wound is closed and leave behind the uncoated suture, so their use is mainly to facilitate the stitching process by reducing the tissue drag. On the other hand, insoluble coatings stay for long periods of time on the suture even after wound closure. They are useful for drug delivery directly to the affected tissue, such as antimicrobial or anti-inflammatory agents. Since this kind of coatings don't disappear, knot security is lower than the one obtained with water-soluble coatings [17].

2.1.4. Drug delivery systems

Sutures are applied directly to the affected tissue; thus, there is a high interest in making them more efficient and helpful in the treatment of the tissue. If the suture is able to deliver a certain agent over time directly to the wound, the healing process is boosted significantly. For this, the polymeric biomaterial used for the suture is enhanced with the addition of bioactive agents that have the capability of releasing in a controlled fashion. This is achieved by modifying the polymerization process in order to get different chemical and physical interactions. Sutures with drug delivery systems are capable of achieving lower risk of site infection, more efficient wound healing, high drug capacity and controlled drug delivery to the site, capacity of introducing extracellular matrix components (proteins, cytokines, anti-microbials, etc.) and sufficient mechanical properties for the wound healing process [18].

2.1.5. Nanofiber coating

A nanofiber coating is added to modify the surface area and the porosity of the suture, this in turn will provide the suture with additional properties such as antimicrobial capabilities, hemostatic capabilities, improved biocompatibility and biodegradability among others [19]. For example, as it is the focus of this project, the addition of a polycaprolactone (PCL)

coating to a regular suture enhances its biocompatibility and biodegradability without decreasing the original mechanical properties of the thread; therefore, usual problems found in absorbable sutures such as inflammation and incorrect scarring are corrected due to the improved biocompatibility [20]. Nanofiber coatings have the potential of improving existing sutures simply by correcting their disadvantages. This is the reason why this field of study is receiving a lot of attention in recent years.

2.2. Electrospinning

Currently, nanofibers are produced by phase separation, drawing, template synthesis, self-assembly, and electrospinning. Out of these five methods, electrospinning is the most common due to its precise control of important properties of the spun nanofiber, such as composition and thickness. This translates into the ability of controlling the porosity of a mesh formed by these nanofibers. This is a possibility because of the direct control of input variables like voltage, distance between collector and nozzle and the flow rate [21]. Additionally, this process is really simple to operate and all its variants have the capacity to be scaled to the industrial level. This process allows for the production of nanofibers from 100nm to 1000nm.

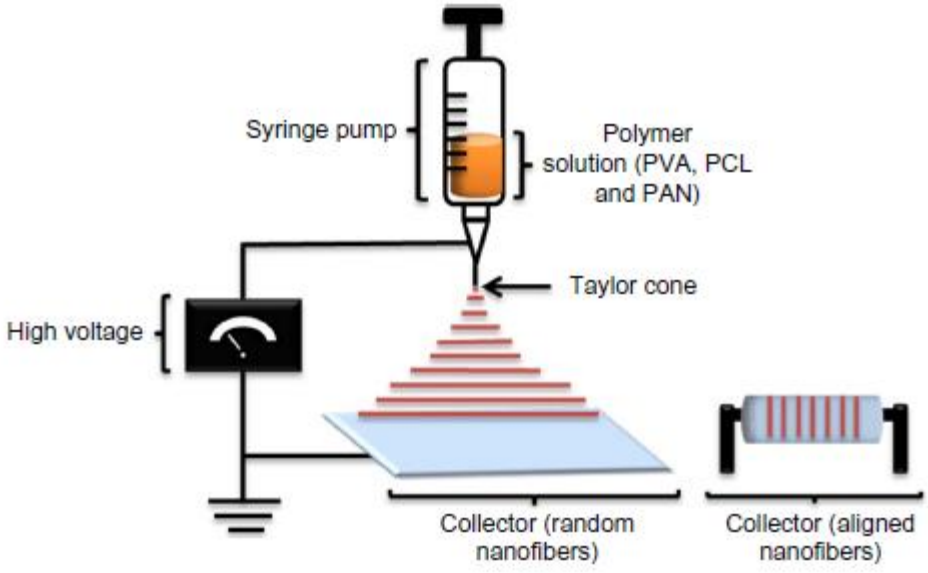

Figure 2.2. *Schematic of a DC electrospinning arrangement* [22]

The electrospinning method has two main variants, needle and needleless. As seen in figure 2.2, the needle variant uses direct current to generate the voltage differential (DC electrospinning). The set up consists of a high-voltage generator, a needle spinneret, the polymer solution and a grounded collector. When the high voltage is applied, electrostatic forces act on the droplet located at the tip of the needle. The polymer solution droplet is charged and changes its shape into a cone (Taylor cone) due to the increase in electrostatic-field intensity. When the critical voltage is met, the equilibrium of forces acting on the Taylor

cone is disrupted resulting in a charged jet being shot out from the tip of the cone in the direction of the collector. In the air, the solvent evaporates and the fibers are elongated to the point where their diameter is in the nanometer scale [21].

The process is affected by a wide variety of factors such as, distance to the collector, flow rate, voltage, solution parameters and environment conditions. Nonetheless, this variant of electrospinning is the easiest one to control. The drawback comes in the form of production rate, in needle electrospinning, one needle generates only one jet. This results in low efficiency in fiber productivity, under 300 mg/h per needle [23]. Additionally, the need of an electrically active collector makes it difficult to combine this variant with other processes due to the presence of a strong electrical field.

To counteract the low production rate of needle electrospinning, research was conducted in order to spin nanofibers from open surface fluids using electric fields. This method is known today as needleless electrospinning and has can be done with a wide variety of arrangements and with different surfaces [23]. Additionally, recent research has shown that changing from a DC to an AC (alternating current) voltage generator further improves the productivity of the process [24].

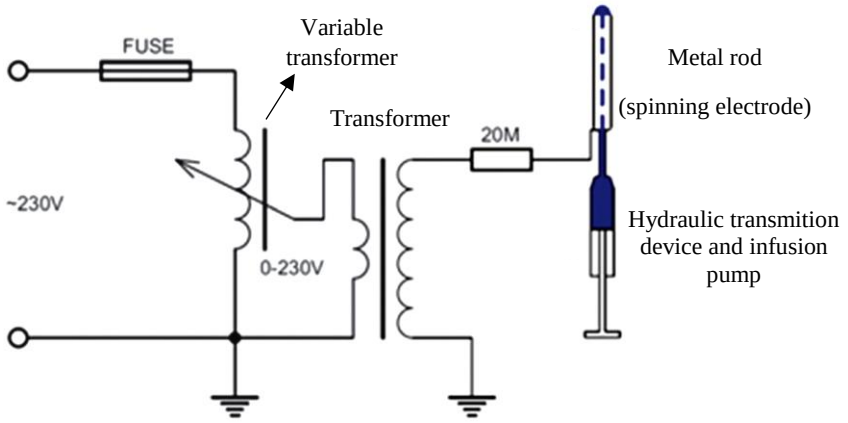

Figure 2.3. *Schematic of an AC electrospinning arrangement* [24]

As seen in figure 2.3, this AC electrospinning arrangement changes the voltage generator for a transformer and a variable transformer, which will be responsible for the alternating current. The needle is replaced for a metal rod that acts as a spinning electrode when the charge is applied. An arrangement of syringes feeds the polymeric solution to the tip of the metal rod with the help of a hydraulic transmission device. In this variant, the nanofibers are carried from the spinning electrode to the neutral collector by the action of the electric wind created

by the alternating of charges in the spinning electrode. The electric wind is a result of the movement of ions generated by corona discharges, the ions are then accelerated by the electric field and transfer momentum to the gas molecules in the vicinity. The solution at the tip of the electrode forms various jets where the solvent evaporates rapidly; thus, forming long strands of nanofibers. It is reported that the forming nanofibers behave like a plume and are easily manipulated and placed on the collector [24]. Additionally, the polymer system that acts as the focus of this diploma project is produced with the goal of being spun with this last version of the electrospinning process. There are efforts being made by the research group directed by professor David Lukas at TUL in projects parallel to this one, where the focus is centered in optimizing the resulting PCL nanofiber coated suture.

2.3. PCL applications

PCL is an aliphatic polyester with a high research value and potential for medical applications in the tissue engineering field. It is obtained by ring-opening of the ε-caprolactone, which happens in the presence of stannous octanoate or similar catalysts. PCL has a glass transition temperature of -60°C, a crystallization temperature range from 34°C to 44°C and a melting point of 60°C [25]. Its chemical composition is shown in figure 2.4.

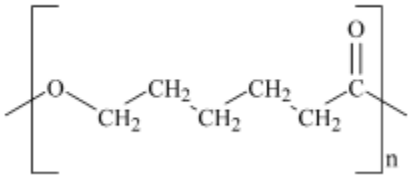

Figure 2.4. *Single segment of a PCL polymeric chain* [25].

This polymer draws attention due to its combination of good mechanical properties, miscibility with a wide variety of polymers, biocompatibility and biodegradability. These properties are dependent on the polymer's degree of crystallinity and molecular weight, which can take a wide range of values. Due to the ester linkages present in this polymer, biological processes are able to hydrolyze these functional groups under normal conditions; thus, the human body is able to degrade the polymer without activating the immune system [5].

In summary, PCL is a hydrophobic, biocompatible and biodegradable semi crystalline polymer with high solubility under normal conditions. Additionally, it is easy to process (low melting temperature and high blending compatibility), which inspired the research of this polymer for a multitude of applications; most importantly, in the biomedical field [26]. Among the main applications that have been studied for PCL are biodegradable drug delivery systems, biodegradable films for packaging, reinforced PCL composites and specialized textile medical devices (sutures and nanofibrous scaffolds for tissue engineering). For this project, the focus is on the specialized medical devices, especially on the inclusion of PCL in sutures. As is the case of the system being studied in this work.

2.4. Sol-Gel systems

Gels have had many definitions through the years, because their behavior is very specific to each case. Due to this, it is beneficial to use a definition that is wide enough to describe most of the known gel systems but narrow enough to separate gels as a specific state that a solution can achieve. In recent years, one of the most adequate definition of gel was given by Tanaka. He stated that a gel is a three-dimensional network composed mainly by polymeric chains, molecules, colloids, other particles and in most cases solvent particles. These composites are interconnected by their functional and associative groups; thus, creating crosslinks. Thanks to these configurations gels have compositions that can be found in liquids but demonstrate mechanical qualities closer to those of solids [27].

This definition is satisfactory for a wide variety of gels; nonetheless, gels can be divided into smaller sub-categories that accommodate better to the most notorious differences found among gels. There are 2 main ways of classifying gels: according to their constituents or their stability over time.

- Classification by constituents[27]–[29].
    - Particulate gels: These gels contain a conglomeration of individual particles or colloids that generate a network.
    - Polymeric gels: Crosslinking happens between primary polymeric chains, generating a stable 3D network.
    - Low-mass gels: The network is created by covalent bonds and van der Waals interactions among low molecular weight molecules.
    - Biopolymeric gels: Crosslinking between biopolymers.

- Classification by stability[27]–[29].
    - Chemical gels: The most stable form of gels. The crosslinks are formed by covalent bonding between primary polymeric chains. The stability is a result of covalent bonds being resistant to the thermal motion inherent to molecules, this allows for the topological structured to be preserved over long periods of time.
    - Physical gels: Also known as thermoreversible gels. The crosslinking is caused by van der Waals forces such as hydrogen bonds and dispersion forces. These are low energy bonds, so thermal energy is enough to separate the molecules; thus, these gels are only stable at low temperatures.

- Other classifications (gels where chemical and physical links co-exist) [28].

    - Transient gels: The network is formed by junctions that are being constantly created and destroyed by thermal motion (physical gel).
    - Sliding ring gels: The network is formed by constant but mobile crosslinks. The junctions are conserved over time; therefore, they can be considered chemical gels.
    - Jamming gels: Viscoelastic fluids with a long relaxation time. The network consists of delocalized crosslinks.

In the case of this project, the studied system can be classified as a thermoreversible or physical gel. Because it becomes a gel when refrigerated and does not require any different input than the change of temperature in order to do the transition. Additionally, this transition is completely reversible and can be done multiple times with the adjustment of temperature. Even with this evidence, the possibility of the system being classified as a transient gel lingers. As the acid solvent system facilitates the hydrolysis of the PCL chains, the newly broken chain ends are then available for the generation of new covalent bonds. The later part is a theory worth mentioning; nonetheless, the system is considered a thermoreversible gel through the whole diploma project.

Additional research on the topic states that there are three possible gelling mechanisms (figure 2.5) acting on the transition from a polymeric solution to a thermoreversible gel. The first mechanism is the classic hydrogen bond association model. Where non-covalent bonds are formed between the polymeric chains due to the extraction of thermal energy. These links between polymer chains are responsible for the sudden increase of viscosity in the system [30]. The second mechanism consists of the polymer crystallite formation. Which states that the polymer crystals form a fringed micelles that swell with solvent and knot around each other forming a 3D structure [31]. The third and final gelation model being considered is based on the liquid-liquid phase separation caused by spinodal decomposition during the gelation process. This model states that by lowering the temperature, the polymeric solution separates into polymer-rich and polymer-poor regions inside the solution. Thus, the 3D structure responsible for the resulting gel is dependent on the level of interconnection among the polymer-rich regions [32]. During the sol-gel transition all three of these models are present in different amounts, which most likely depend on variables from the specific system, such as polymer and solvent properties, and variables from the gelation process, especially the temperature at which the polymer is being stored.

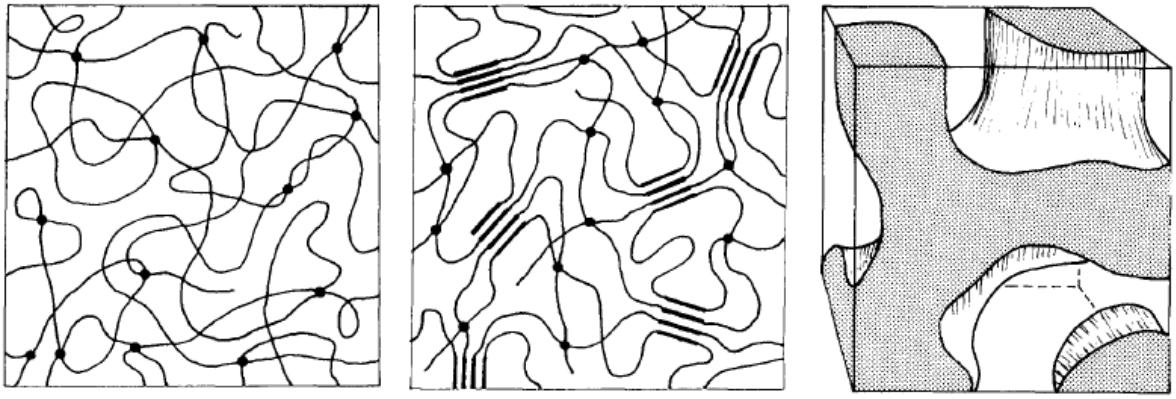

Fig 2.5. *3D polymeric network formed by:* ***(a)*** *hydrogen bond association* ***(b)*** *crystallite formation* ***(c)*** *interconnected polymer-rich regions after spinodal decomposition* [30].

2.5. Finding the sol-gel transition temperature

In the literature there is not a universally effective method capable of defining the sol-gel transition point for every thermoreversible gel. This is due to the fact that every physical gel has greatly varying properties and characteristics that depend on variables coming from the macromolecules, solvents and other components present in the system, as well as their respective interactions with each other. Nonetheless; the general idea used in most methods take advantage of the rheological differences shown by the system in its gel state compared to the ones shown in its solution form. The following are some examples used as inspiration for the experimental work carried out in this diploma project.

The most common rheological method is called the tube inversion test (figure 2.5), which is carried out by turning upside down a tube containing the sample. This test is based on the assumption that the sample will resist flow in its gel form, while flowing noticeably once it returns to its solution form [33]. The main issue with this test is that when studying a new system, it is easy to confuse a high viscosity solution with a low viscosity gel. Additionally, with highly viscous samples the flow rate may be too slow for the correct identification of the transition temperature. Therefore, this method is used mostly in the detection of gelation, rather than in the precise identification of the gelation point.

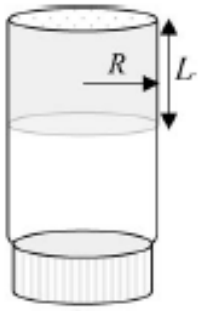

Fig 2.6. *Schematic of the tube inversion test with the gel at the top of the illustration* [33].

Another source of inspiration comes from the method developed by Harrison et al in 1971 for identification of the transition temperature in sol-gel systems [34]. In this article the authors describe an apparatus designed to the detect the flow of the system through a capillary tube in U-shape, as seen in figure 2.7. There would be a different level of the gel on each arm of the apparatus to ensure the onset of flow once the system returned to its solution form. This was done by increasing the temperature of the whole system at a controlled and constant rate. One of the drawbacks of this method is the restriction of it only working reliably with low rigidity modulus gels. Additionally, the calibration of the apparatus and its variables are dependent on the gel being studied. Variables such as the diameter of the capillary and the difference in level between the two arms are to be determined by trial and error for each new system being studied.

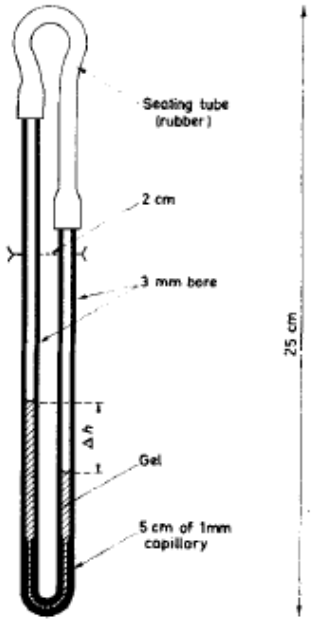

Fig 2.7. *Schematic of the apparatus developed by Harrison et al. The apparatus consists of a glass of constant diameter in the limbs, a capillary tube at the bottom and a rubber sealing tube* [34].

2.6. Mathematical model

To further describe and understand the polymer-solution system that is in the spotlight of this diploma project, it is necessary to predict its behavior by finding and accommodating a mathematical model that closely fits the real behavior of the system, as well as providing a better understanding of the physicochemical aspects of the system. The inspiration for this mathematical model and its development is found in the book published in the Czech language by Prof. David Lukas et al [35].Since the main goal is to study the sol-gel transition temperature, the objective of the mathematical system will be to obtain the behavior of the transition temperature as a dependent variable of the concentration of polymer in the system. To accomplish this, we have to start with the definition of the change in free energy of the system with the inclusion of temperature term that will allow us to express the transition temperature in terms of other variables such as the concentration of the polymer or the solvents.

$$\Delta F = \Delta U - T\Delta S \qquad (2.1)$$

Where ΔF is the change in free energy of the system, ΔU is the change in internal energy of the system, T is the general temperature at which the solution is at the specified moment and ΔS is the change of the thermodynamic entropy in the closed system. The thermodynamic entropy (S) can be related to the statistical entropy (σ) in the following manner, where k_B is the Boltzmann constant.

$$S = k_B\sigma \qquad (2.2)$$

The first step we will take in developing equation (2.1) will be to expand the entropy term of the right-hand side by introducing a lattice model, with an *n* number of total nodes that allows us to simulate a basic version of the forming of a polymer-solvent mixture. For this we will assume the Pauli principle of indistinguishability of identical particles applies for the solvent in the system. This principle states that identical particles in a big system are interchangeable but impossible to be distinguished experimentally [36]; thus, the resulting configurations of interchanging just solvent molecules are to be considered as one configuration. One possible outcome of the mixing is shown in figure 2.8.

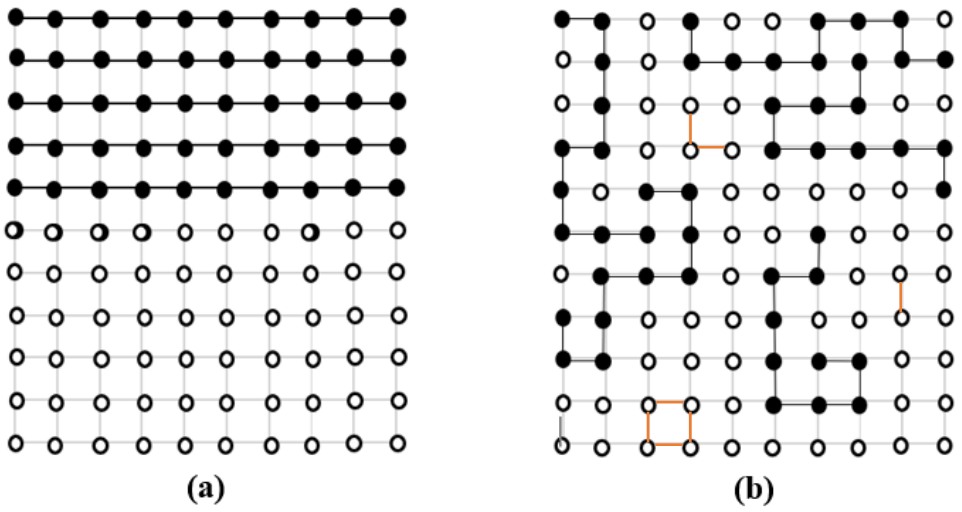

Fig 2.8. (a) *A system of polymer molecules and solvent molecules before mixing* ***(b)*** *One of the many possible configurations of the same system after mixing with the apparition of solvent clusters denoted by red lines.*

With a model like the one shown in figure 2.8 it is possible to describe the mixing of the system in terms of the change in statistical entropy (Δσ) which in turn, depends on the number of possible configurations of the polymer-solvent system in the presented lattice model. Because of the following relation where g is the total number of possible configurations of the system.

$$\sigma = \ln(g) \qquad (2.3)$$

The change of statistical entropy of the whole system can be expressed as the total of the sum of the change in particle entropy for each particle inside the system. As the particle statistical entropy (σ') is defined as the number of places where a particle or polymer center of mass (or polymer center of mass) can be located.

$$\Delta\sigma = n_p\Delta\sigma_p' + n_s\Delta\sigma_s' \qquad (2.4)$$

Where n_p is the number of polymer chains, $\Delta\sigma_p'$ is the change in statistical particle entropy per polymer chain, n_s is the number of solvent clusters and $\Delta\sigma_s'$ is the change in statistical particle entropy per solvent cluster. From the interactions between solvent molecules in this specific system it is expected to find solvent clusters where 2 or more solvent molecules join with Van der Waals forces. Nonetheless, by focusing in the change of entropy per particle, this allows us to assume that every individual particle will occupy a specific node inside the lattice model.

Now the change in particle statistical entropy is estimated for the polymer chains and the solvent clusters in terms of their own numerical fractions, ϕ_p for the polymer segments and ϕ_s for the solvent clusters. For numerical fractions holds the following relations.

$$\phi_p = \frac{n_p N}{n} \quad (2.5)$$

$$\phi_s = \frac{n_s c}{n} \quad (2.6)$$

Changes in statistical entropy per one particle are the following.

$$\Delta\sigma_p' = \ln(n) - \ln(n_p N) = -\ln\left(\frac{n_p N}{n}\right) = -ln\phi_p \quad (2.7)$$

$$\Delta\sigma_s' = \ln(n) - \ln(n_s N) = -\ln\left(\frac{n_s c}{n}\right) = -ln\phi_s \quad (2.8)$$

Where *N* is the degree of polymerization of the polymer chains and *c* is the average size of the solvent clusters. This means that the total number of molecules in the system can be estimated in the following way.

$$n = n_p N + n_s c \quad (2.9)$$

By adding equation (2.7) and equation (2.8) in equation (2.4) we get.

$$\Delta\sigma = -n_p ln\phi_p - n_s ln\phi_s \quad (2.10)$$

$$\frac{\Delta\sigma}{n} = -\frac{\phi_p}{N} ln\phi_p - \frac{\phi_s}{c} ln\phi_s = -\frac{\phi_p}{N} ln\phi_p - \frac{(1-\phi_p)}{c} ln(1-\phi_p) \quad (2.11)$$

The following step is to unravel ΔU, which is done by first describing the energy that polymer segment-solvent molecule (ε_{ps}) bonding takes away, after mixing, from the energy polymer-polymer (ε_{pp}) and solvent-solvent (ε_{ss}) bonds poses before the mixing. Equation 2.12 describes this situation.

$$\Delta\varepsilon = \frac{1}{2}\left(\varepsilon_{pp} + \varepsilon_{ss} - 2\varepsilon_{ps}\right) \quad (2.12)$$

Following equation (2.12), this can define $\Delta\varepsilon$ as the energy of forming one p-s bond. So, to find the total energy change, it is necessary to calculate how many of these bonds are formed in total. These bonds are formed based on the amount of number of polymer segments that end up surrounded by solvent molecules. The total number of polymer segments is given by $n\phi_p$, while the average number of adjacent solvent segments is $z(1-\phi_p)$, where *z* is the coordination number (4 in the case of a 2D model, 6 for a 3D model). So, the total number of p-s bonds (n_{ps}) formed after mixing can be expressed as eq 2.13. And introducing the interaction parameter between solvent and polymer in eq. 2.14.

$$n_{ps} = n\phi_p z(1-\phi_p) \quad (2.13)$$

$$\chi = \frac{z\Delta\varepsilon}{k_B T} \quad (2.14)$$

Based on equation (2.13), ΔU is expressed as it follows. Subsequently, it is mixed with equation (2.14).

$$\Delta U = n\phi z\left(1-\phi_p\right)\Delta\varepsilon = nk_BT\phi_p(1-\phi_p)\chi \qquad (2.15)$$

The change of internal energy per node is then expressed as equation (2.16).

$$\frac{\Delta U}{n} = k_BT\phi_p(1-\phi_p)\chi \qquad (2.16)$$

Now it is possible to find the free energy per node by putting eq 2.11 and 2.16 together.

$$\Delta f = \frac{\Delta F}{n} = \frac{\Delta U}{n} - \frac{T\Delta S}{n} = k_BT\left(\frac{\phi_p}{N}ln\phi_p + \frac{(1-\phi_p)}{c}\ln\left(1-\phi_p\right) + \phi_p(1-\phi_p)\chi\right) \qquad (2.17)$$

$$\frac{\Delta f}{k_BT} = \frac{\phi_p}{N}ln\phi_p + \frac{(1-\phi_p)}{c}\ln\left(1-\phi_p\right) + \phi_p(1-\phi_p)\chi \qquad (2.18)$$

Equation (2.18) is the base Flory-Huggins expression derived for this specific case of polymer-solvent mixing. Finally, the equation that better describes the temperature at which the gel forms using the spinodal decomposition mechanism is found by localizing the inflection points present in the Flory-Huggins curve. Therefore, the second derivative is calculated and made zero $\left(\frac{d^2f}{d\phi^2} = 0\right)$ in order to get an expression of the temperature of the system in dependance on the concentration of polymer in the inflection points of the curve. This spinodal expression is shown as equations (2.19) and (2.20).

$$\chi = \frac{1}{2}\left[\frac{1}{N\phi_p} + \frac{1}{c(1-\phi_p)}\right] = \frac{z\Delta\varepsilon}{k_BT} \qquad (2.19)$$

From here one easily obtains.

$$T = \frac{z\Delta\varepsilon}{k_B}\left[\frac{2Nc\phi_p(1-\phi_p)}{c(1-\phi_p)+N\phi_p}\right] \qquad (2.20)$$

Nonetheless, an additional term dependent on the square of fraction of polymer, ϕ^2 and temperature was suggested due to the discrepancy between experimental data obtained by us and theoretical results obtained by Tanaka [27]. This term is entropic in nature and represents the different number of configurations that individual polymeric chains realize before and after the mixing of the system happens. In fact, this factor can be attributed to the conformation restrictions coming from the gel forming mechanisms, e.g. hydrogen bond association and parallelization of polymer chain parts thanks to crystallite formation. Nonetheless, we hypothesize that these two additional mechanisms are not considered in the derivation of the original model, when spinodal decomposition is being considered as the driving force of the gel phase formation by most authors, such as Tanaka and Kawanishi. Resulting in a more robust and complex Flory-Huggins equation (2.21).

$$\frac{\Delta f}{k_BT} = \frac{\phi_p}{N}ln\phi_p + \frac{(1-\phi_p)}{c}\ln\left(1-\phi_p\right) + \phi_p(1-\phi_p)\chi + G\phi_p^2 \qquad (2.21)$$

Finally, equation (2.21) is derived two times and equaled to zero in order to obtain a more reliable spinodal model to use as a mathematical model, found in equation (2.22).

$$T = \frac{z\Delta\varepsilon}{k_B}\left(\frac{2Nc\phi_p(1-\phi_p)}{c(1-\phi_p)+N\phi_p+2GN\phi_p c(1-\phi_p)}\right) \tag{2.22}$$

Where *G*, *N* and c are unknown values, *T* is the dependent variable, ϕ_p is the independent variable and the values for the constants required to in the mathematical model were obtained from the literature and are the following [37].

$$\frac{\Delta\varepsilon}{k_B} = 0.7$$

$$z = 6$$

3. EXPERIMENTAL WORK

This chapter will talk about the new concepts and techniques this study and similar studies carried out in TUL bring to the table when it comes to the topic of PCL nanofibrous coatings for surgical sutures.

3.1. PCL in sutures

High biocompatibility is the key factor that allows PCL to be implemented in new and upgraded versions of previous medical devices that are required to have a direct interface with the tissue they are treating. Currently commercialized sutures based on aliphatic polyesters face one major drawback. Sutures made from materials such as polylactic-polyglycolic acid (PLGA), polyglycolic acid (PGA) and polydioxanone (PDS) generate a suboptimal inflammatory response due to their invasive nature on cell activity [38]. With the introduction of PCL nanofibers, this drawback can be reduced; thus, adding value to the suture in question.

3.2. PCL in mixture of acetic acid, formic acid and acetone

As mentioned above, PCL is a polymer that is relevant for various applications in the medical textiles field. Which turns it into a highly studied material in the field. The process that is going to be applied to the PCL to obtain nanofibers is electrospinning. For this, the PCL will have to be dissolved in a non-toxic compatible solvent system. A mixture of FA and AA is known to be a good solvent system for PCL, resulting in a spinnable viscous solution. The one problem present in this system is the hydrolytic degradation of the PCL due to the effect an aqueous acidic media has on a polyester [39].

To counteract this effect, the research group directed by Prof. David Lukas added At to the solvent system, due to the fact that At is another non-toxic solvent that has shown promising results with PCL [40]. In addition, to further slowdown the degradation process of the PCL, the system was stored in a freezer that reaches temperatures under -10°C. In this storage, the research group discovered how the solution formed a thermoreversible gel and the degradation was successfully stopped. This phenomenon can be explained by the expected lowered reactivity of the system in the gel phase. The reaction kinetics are significantly slowed down by lowering of the diffusion of the different components of the system as well as the entanglement of the polymeric chains once the gel phase has been formed successfully [41]. Thus, creating the motivation to study more closely the behavior of this system around the sol-gel transition point.

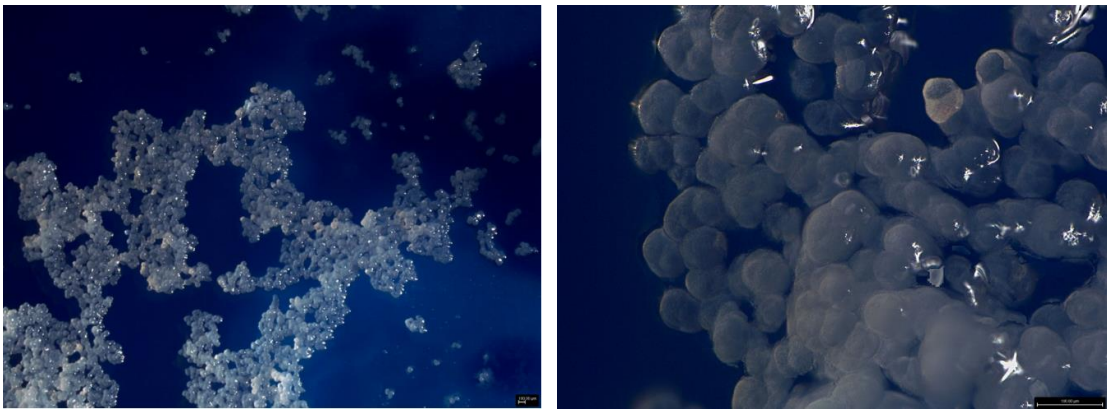

Fig 3.1. *Microscope images of the gel phase of a 10% PCL in AA:FA:At sample taken with the Leica DVM6 digital microscope.*

Figure 3.1 shows a close-up microscopic image taken with the help of E. Kuželová Košťáková using a Leica DVM6 digital microscope. The scale in the bottom right corner of both of these images is of 0.1 mm. These images show a very interesting aggrupation of spherical and smooth PCL microparticles in the form of a 3D structure. By forming these 3D structures, the gel phase of the system is obtained.

3.3. Sol-Gel transition

As explained before, the system that is being studied is a PCL containing thermoreversible gel that requires refrigeration to remain stable and not degrade the polymer. This way the hydrolysis of the PCL is stopped thanks to the inert nature of the solvent system in gel form. An additional discovery done by the same research group was that the gel form of this system has really good spinnability properties. Thus, highlighting the importance of finding the specific sol-gel transition temperature to optimize the storage requirements of this specific system.

3.4. Sol-Gel transition temperature

Due to the previously stated importance of this parameter, and the projection of PCL as a highly relevant material for the future of medical textile and the general nanomaterials field of study; a great effort was made during this diploma project to design a method capable of identifying the transition temperature with accuracy for the PCL-AA:FA:At system and other similar polymeric solutions. As stated above, one of the main observable differences between the gel and solution phases for this system, are their rheological and visual characteristics. With the gel phase being an opaque, white and thick semisolid with a high resistance to flow, while the solution phase is a translucent liquid with low viscosity. The experimental methods were designed with this difference in mind, initially in a qualitative way based loosely on observation of the system while it transitions from one phase to the other.

4. MATERIALS AND METHODS

This chapter is dedicated to mentioning the materials and methods used during this diploma project, as well as clarifying the experimental process that took place in order to arrive to the results and conclusions, which will be shown in detail in the following chapters. As mentioned above, the solution to be studied consists of the following chemicals.

- PCL of Mn 80000 provided by Aldrich chemicals.
- 98% formic acid of analytical grade from Penta chemicals.
- 99% acetic acid of analytical grade from Penta chemicals
- Acetone of analytical grade from Penta chemicals.

These chemicals were acquired previously for another research project using the same polymeric solution. These chemicals were used as they came from the provider.

For the last experimental set-up, a thermometer model GMH 3210 with K-type probes from the Greisinger brand was used in the temperature measurements. And a laser model Sios SL04/A from the SIOS brand was employed for the latter laser set-up of the experiments. Additionally, a PDA10A photodiode from Thorlabs was used as a receptor of the laser signal in the last experimental set up.

Fig 4.1. *Thermometer, laser and photodiode used in the final experimental set up.*

4.1. Solution preparation

A multitude of solutions with different concentrations of PCL and the solvents were prepared using the same process; described in the following text. A mixture of the solvents (AA, FA) is prepared at room temperature while the required PCL is weighted separately. Consequently, the PCL is added slowly to the solvent mixture while it is being stirred by magnetic stirrer at medium speed. Once all the PCL has been added and partially dissolved, the Ac is added and the stirring speed is increased. The sample is left alone until it becomes a homogenous solution. To ensure the complete dissolution of the PCL, the samples were stirred overnight for 24 hours at 35°C and 1000 rpm stirring speed using a 1 cm long magnetic stirrer. Afterwards, the samples were always refrigerated to avoid depolymerization and contained in a closed vessel to avoid the rapid evaporation of the solvent.

4.2. Sol-Gel transition temperature study

Based on the methods and proposals found in the literature, a set of experiments were designed based on the initial observations and subsequent results obtained. With each iteration, a more accurate and robust method was proposed. Culminating in a satisfying experimental set-up that can be used as the foundation of follow up studies regarding the precise identification of the transition temperature of thermoreversible gels.

4.2.1. Initial flow experiments

The first step was to use the inverted tube method to understand the rheological difference between the gel phase and the solution phase of the system. A glass vial containing a sample of 10%(w/vol) PCL in a 1:1:1 ratio solvent system was stored in the freezer for 45 minutes, obtaining a white and opaque gel. The vial is then taken out of the freezer, turned upside down and exposed to room conditions (22°C) until the white gel transitioned into a translucent solution phase, as shown in figure 4.2. With the observations done in this initial experiment it was possible to choose a direction to follow for the design of the follow-up tests.

Fig 4.2. *Inverted tube with sample in gel phase at the top of the set-up.*

Since the onset of flow was visible, the following experiment was designed with the objective of finding an accurate way of identifying the transition temperature between these two phases. A plastic micropipette tip was used as a container for the sample and stored in the freezer in order to obtain the gel phase of the system, the thermometer probe was placed in the middle of the sample with the intention of measuring the temperature profile through the

whole transition. Since the objective of the experiment is to observe the temperature when the onset of flow happens, the micropipettes were placed vertically, with the thermometer probe already inserted, and exposed to the normal conditions of the laboratory in order to increase the temperature of the system gradually (figure 4.3).

The experiment was done with 5 mL, 1 mL, 0.2 mL and 0.05 mL micropipettes to corroborate which size would allow for a fast enough flow that could be identified, but not fast enough that the contents of the micropipette would be emptied too fast for a valid measurement. Each micropipette size was tested three times, in order to discard possible effects caused by factory defects from an individual unit.

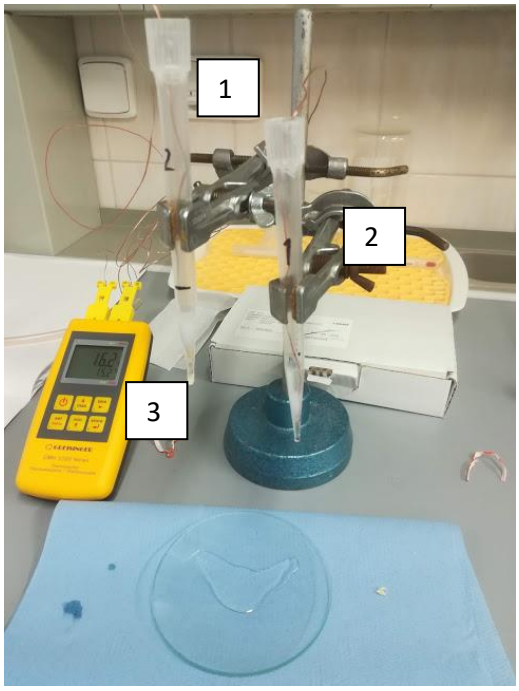

Fig 4.3. *Micropipette experimental set-up. It consists of (1) Sample containing micropipette with K-type thermometer probe (2) vice grip for vertical stabilization and (3) thermometer.*

As it will be discussed in more detail in the following chapter, these initial flow experiments were not successful in identifying accurately the transition temperature of the PCL sample. Nonetheless, they were useful in understanding the principles of this phase transition and planning the following steps in order to design an accurate set up capable of carrying out this measurement.

4.2.2. U-shaped tube

Based on the transition temperature determination method proposed by one of the sources of this diploma project [34], a U-shaped tube was designed by the combination of 0.5cm in diameter and 16cm in length glass tubes with a 0.5cm in diameter and 10.5cm in length silicone hose section (figure 4.4). The principle behind this design was to fill the arms of the

tube with an uneven level of the PCL sample, a known Δh of 5cm and store the apparatus containing the sample in the freezer until the transition to gel occurred. After this event, the temperature was measured with the GMH thermometer probe in the silicone hose section in order to find the temperature at which the Δh of the level in the arms would start decreasing. Since this disappearance of the Δh would mean that the sample transitioned back into its solution phase. For this experiment, the transition temperature was measured five times for the same PCL sample used in the previous iterations.

Fig. 4.4. *U-shaped tube experimental set-up. Where the limbs are glass tubes of constant diameter, the bottom is a silicone section containing a K-type thermometer probe and on the top there is a silicone sealing.*

The above-mentioned apparatus was an idea worth exploring, but as it will be explained in the next chapter, this experimental set-up did not meet the expected results and instead was another step towards the development of more ideas.

4.2.3. Visual identification

Since the onset of flow experiments did not yield satisfactory results, a new approach was taken to study the sol-gel transition of this PCL-solvent system. This new approach is based on the principle that the sol-gel transition of this system is clearly observable, even by the naked eye. Therefore, a basic and quantitative method was designed to measure the temperature of the system while the sample is under careful observation. The objective of this first set up was simply to determine if this more quantitative method showed promise in the accurate pinpointing of the transition temperature of this system. The set up consisted of

the GMH thermometer, the K-type probes and a glass vial containing 10mL of the previously-cooled gel form of the sample (figure 4.5).

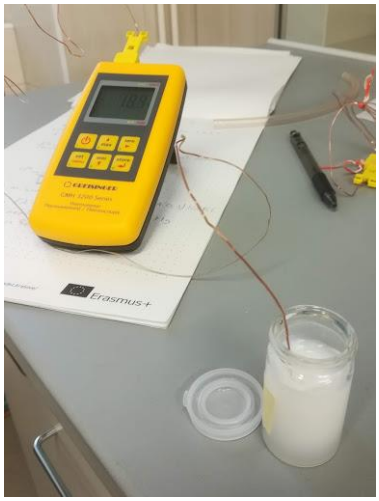

Fig 4.5. *First visual experiment set-up with glass vials with a K-type thermometer probe inside the vial and connected to a thermometer.*

The set up shown in figure 4.5 provided a good starting point for the identification of the sol-gel transition temperature of the PCL system by making use of the drastic difference in opacity and color between the two phases of the system in question. The following step in the design and correction of this technique was to increase its accuracy. This was initially done by reducing the size of the vial from 10 mL to roughly 1.5 mL by using snap-cap Eppendorf tubes. The process was the same as in the first iteration, the Eppendorf containing the sample in gel phase was stabilized and the K-type probe of the thermometer was inserted in order to observe the temperature profile as the transition took place. The temperature was written down as soon as the observer determined that the transition took place based on the visual cues given by the change in appearance in the sample.

Fig 4.6. *Second iteration of the visual experiments using Eppendorf tubes and a K-type thermal probe connected to a thermometer.*

The size decrease proved to be the right way in terms of data collection efficiency and visual clarity. Nonetheless, the Eppendorf tubes did not satisfy the repeatability requirement of an experiment, thus a new iteration of the experimental set up was proposed in order to correct this crucial drawback. The third iteration of this set up used 5 mL and 1 mL micropipettes as containers for the sample in gel phase, as seen in figure 4.7. By implementing 1mL micropipettes, this iteration showed an increased repeatability of the results with a less tedious set-up when compared to the Eppendorf tube iteration of this experiment. The new experimental set-up follows the same process shown before. The micropipette is stored in the freezer with the PCL solution sample and an already inserted K-probe from the thermometer to force the transition of the system into the gel phase. The next step was to observe the transition from gel to solution at normal laboratory conditions and write down the temperature where the change was detected.

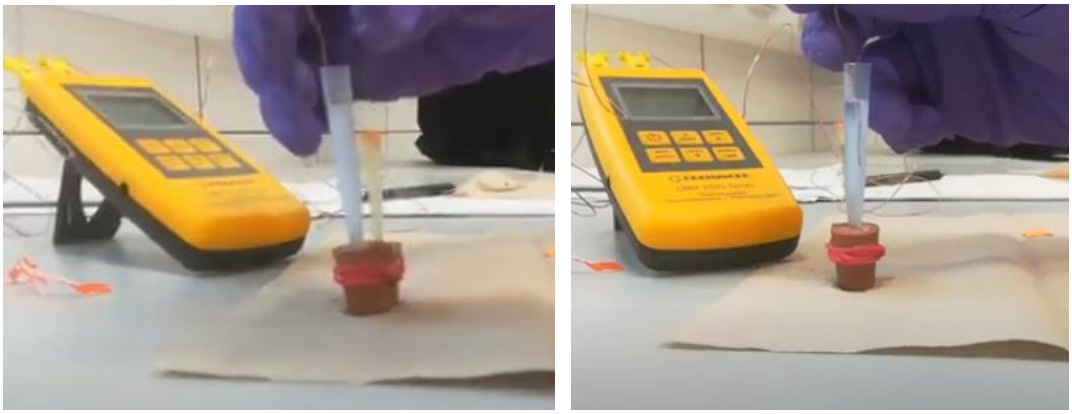

Fig 4.7. *Third iteration of the experiment using 1mL and 0.2mL micropipettes connected to a thermometer via a K-type probe.*

Given that this iteration of the experimental set-up yielded results with a better repeatability, additional effort was put into finding a more reliable vessel with better observation attributes and an easier to operate geometry. With these objectives in mind, the fourth and final iteration of this series of experimental set-ups gave way for the inclusion of rectangular, transparent acrylic vials (figure 4.8). These new sample containers allowed for a more standardized way of preparing the sample and observing the transition take place. Again, this set-up requires the solution to be poured into the acrylic vial to be stored in the freezer to ensure the phase transition to gel. Once taken out from the cold storage, a K-type probe from the thermometer is used to follow the temperature as the sample warms back up and transitions back into its solution form. The third and fourth iterations were tested at the same time using six samples of the standard 10% PCL solution.

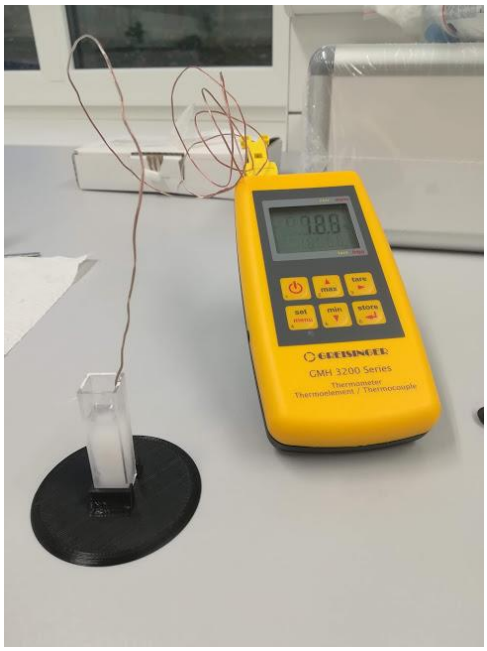

Fig 4.8. *Fourth and final iteration of the visual experimental set-ups with an acrylic vial with the insertion of a K-type probe feeding data to a thermometer.*

After being satisfied with the optimization of the vessel for the observation of the sample, the next step to be taken was to find a more reliable way of observing the transition related visual changes in opacity and color of the system. In other words, replacing the human observer for a mechanism capable of giving quantitative proof that the transition happened while recording the temperature with the thermometer.

4.2.4. Laser-Thermometer set-up

Replacing a human eye was not easy task, but thanks to the collaboration with S. Kunc. from the Department of Physics, PF TUL, we were able to piece together a satisfying mechanism capable of observing the visual transition from an opaque and white gel to a translucent solution. Additionally, this last set-up is able to record in a quantitative way the transition happening, giving room for a better understanding and analysis of the process. The breakdown of how this was achieved is the following. A Sios SL04/A model laser in combination with a PDA10A model photodiode were used as the observer. The laser generates a highly focused beam of light with a wave length around 630 nm, which is aimed at the photodiode with a wave detection range between 200 nm to 1100 nm. Between the laser and the photodiode, the gel phase of the sample is located in a transparent acrylic vial as seen in figure 4.9.

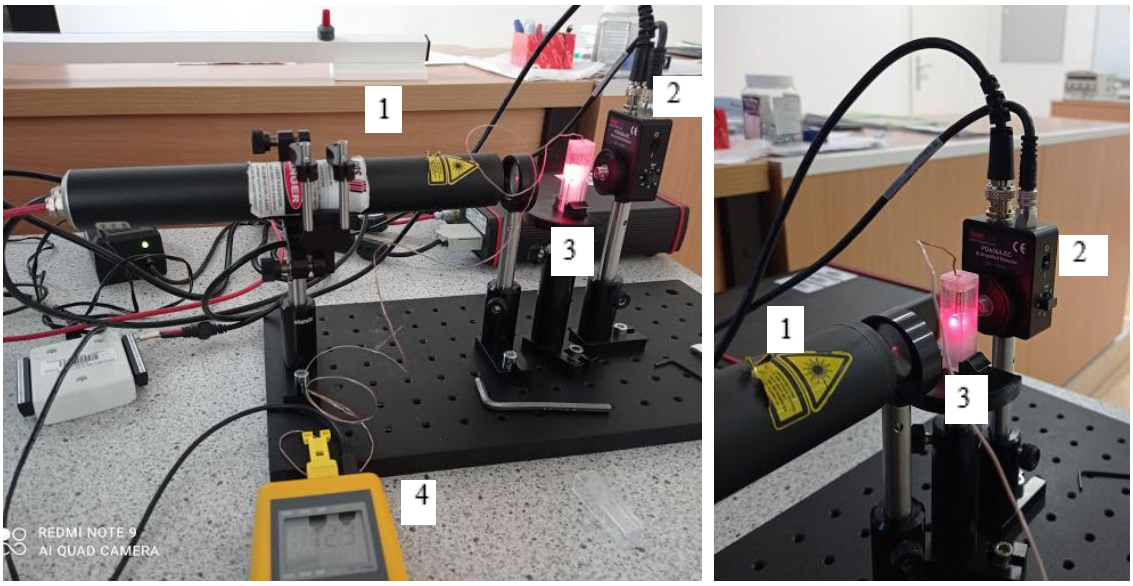

Fig 4.9. *Close up on the laser/photodiode set-up with a PCL sample. Consisting of (1) Laser (2) photodiode (3) acrylic vial containing a PCL sample with a K-type thermal probe attached and (4) thermometer.*

By adding inserting the K-type probe from the GMH 3210 model thermometer into the sample, it became possible to have a record of the temperature profile for the whole observation time. This means that the photodiode worked by taking the incoming wavelength that went through the sample and outputting it as measurable and recordable voltage, while the thermometer recorded the temperature of the sample for the as long as it's needed. Therefore, specialized software was necessary in order to be able to record the data that came from the photodiode and the thermometer.

On the first hand, to be able to get the photo signal given by the photodiode, a computer with the specialized software labVIEW was required. In this software the voltage output (mV) coming from the photodiode was recorded every 0.1 seconds. On the other hand, for the thermometer data collection, a computer with the specialized software VeePro was employed. With this software, the signal coming from the thermometer (°C) was recorded every 0.143 seconds. As a result of the implementation of these specialized softwares, the experimental set-up shown in figure 4.10 was completed.

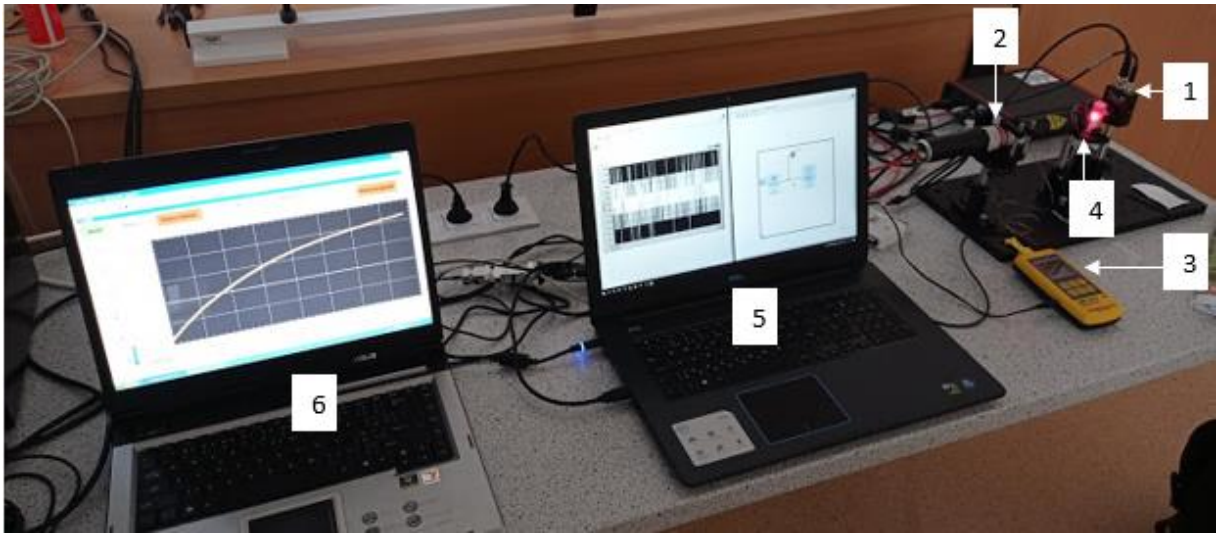

Fig 4.10. *Complete experimental set-up with: (1) PDA10A photodiode (2) SL04/A laser (3) GMH 3210 thermometer (4) PCL-AA:FA:At sample (5) Computer with specialized software LabVIEW (6) computer with specialized software VeePro.*

4.3. PCL/Acetone concentration effect on the transition temperature

Transition temperature is dependent on the concentration of the polymer in the sample, as seen in the mathematical model presented in the second chapter. Using the experimental set-ups that produced repeatable results, it was possible to study this effect closely. The selected methods are the third and fourth iteration from the visual identification experimental set-ups, found in figures 4.7 and 4.8 respectively. As well as the more promising Laser-Thermometer apparatus shown in figure 4.10.

First, for the PCL concentration variation study, the samples were prepared using the same process described in numeral 4.1, using a solvent system of equal parts AA, FA and At and weighting the required PCL to ensure the w/vol concentrations seen in table 4.1. The following concentrations were chosen due to the fact that samples with lower or higher concentrations of PCL did not show the correct formation of the gel phase.

Table 4.2. *Samples used in the PCL variation study.*

Sample number	PCL Fraction(w/vol)
1	0.06
2	0.08
3	0.1
4	0.12
5	0.14
6	0.16
7	0.18
8	0.2

Subsequently, the At concentration variation experiment was designed following a similar process as the one described in numeral 4.1. In this case, the solvent system consisted of AA:FA on a 1 to 1 ratio, while the PCL was kept at 10% (w/vol) for all the samples and the volume fraction of At in the total solution was varied as shown in table 4.2. Due to the same circumstances observed with the PCL study, lower and higher concentrations than the ones found in table 4.2 were not usable.

Table 4.2. *Samples used in the PCL variation study.*

Sample number	PCL Fraction(w/vol)
1	0.15
2	0.2
3	0.25
4	0.3
5	0.35
6	0.4

The results obtained from these measurements will be used to test the mathematical models proposed in equations (2.20) and (2.22) in order to evaluate their capability to predict the behavior of the real system and discuss if which model is better suited to understand the properties of a complex system like the one being studied in this diploma project.

5. RESULTS AND DISCUSSION

This chapter contains the results obtain from the experiments described in the previous chapter, as well as a discussion and analysis based on the data obtained and the studied principles.

5.1. Solution preparation

Once the solution is prepared with the desired PCL, AA, FA and At concentrations, a translucent solution is obtained. As shown in the following image. In order to go through the gel transition, the solution is placed in a freezer. After a period of time of around 45 to 60 minutes a smooth, white and viscous gel is obtained.

Fig 5.1. *On the left, resulting solution of dissolving PCL in AA:FA:At solvent system. On the right, resulting gel from storing the same solution in a freezer for over 45 minutes.*

5.2. Sol-Gel transition temperature study

A series of experimental set-ups that allowed for the closer inspection and better understanding of the transition experimented by the system of interest. The efforts put into this experimental path were rewarded with an interesting new proposal for the study of sol-gel phase transitions, as well as a state-of-the-art experimental set-up.

5.2.1. Initial flow experiments

The experimentation begun with the inverted tube test to better understand if the rheological change observed during the transition is a viable way of further studying the sol-gel transition of the PCL-solvent system. The test is shown in the following figure.

Fig 5.2. *Inverted tube with* ***(on the left)*** *sample in gel phase and* ***(on the right)*** *sample after 10 minutes and the onset of flow.*

As seen in figure 5.2, the sample went from a flow resistant semi-solid gel, to an inelastic liquid solution over a short period of time (time here). The simplicity of this experiment was a great advantage and at the same time its main drawback, due to the fact that with this simple set-up it was not possible to identify the sol-gel transition temperature. Nonetheless, the result of this test indicated that the rheological transformation observed over the course of the phase transition showed potential as an indicator to find the specific sol-gel transition temperature of the system.

A new experimental set-up was designed using micropipettes of varying sizes as explained in numeral 4.2.1. The results of these trials are shown in the following table.

Table 5.1. *Micropipette size experiment results.*

Size (mL)	Flow onset
5	yes
5	yes
5	yes
1	yes
1	yes
1	yes
0,2	no
0,2	yes
0,2	yes
0,05	no
0,05	no
0,05	no

Table 5.1 shows that the bigger 5 mL and 1 mL variations had no issues with the flow onset of the sample during the phase transition. On the other hand, the smallest variation of the

micropipettes did not show any flow at all, this can be explained by the capillary action a container that small has over a viscous liquid such as the 10% PCL solution. In the case of the 0.2 mL size micropipettes, the onset of flow was present; however, an almost indistinguishable defect in the mouth of one of the micropipettes generated enough capillary action in order to keep the solution from flowing after the phase transition was completed. Which is why both of the smaller sizes were discarder for the temperature measurement experiments with this set-up.

Table 5.2. *Micropipette transition temperature experiment results.*

Size (mL)	T. Temp (°C)
5	3,1
5	-1,2
5	9,5
1	10,2
1	5,8
1	-3,6

The results from the transition temperature measurements are shown in table 5.2. As it can be seen from the presented data, these results are not satisfying due to the low repeatability that can be observed within them. Their random nature can be attributed to some unexpected system behaviors. For example, in some cases the transition would be completed in the middle section of the micropipette, while the tip section would still show some gel remnants blocking the mouth and impeding the flow to happen at the opportune moment. It is due to these variations that a new geometry was sought for the next iteration.

5.2.2. U-shaped tube

Next, a tube in the shape of a U made from glass and silicone sections was put to the test with the expectation of it yielding better results than the previous iterations of these set of experiments. Unfortunately, despite the various attempts at making it work, this new apparatus presented similar flaws to the ones observed in its predecessor with the micropipettes. Initially, the thermometer probe was placed to record the temperature in one of the arms (glass section) of the apparatus. The first observation confirmed that the transition occurred much faster in the glass sections when compared to the silicone section of the apparatus. After relocating the thermometer probe to the silicone lower section of the tube, a series of temperature measurements were carried out in order to test the accuracy of this experimental set-up.

Table 5.3. *U-shaped tube transition temperature experiment results.*

Sample	T. Temp (°C)
1	9,3
2	2,1
3	0,4
4	5,2
5	1,1

The results given by these measurements (table 5.3) suffer from a high variability and low repeatability. When comparing this set-up with the one observed in the article used as inspiration for the U-shaped tube [34], there are some key differences that might explain why these results are not satisfactory. In the original apparatus, the tube is made of a continuous glass section, with U shaped part at the bottom being a capillary with lower diameter than the rest of the tube. Additionally, the set-up in the article allowed for a steady and constant control of the temperature through the whole apparatus. Therefore, in order to be able to measure the correct sol-gel transition temperature, there needs to be complete control of the temperature of the system through the whole measurement phase. It was not possible to achieve this condition with the equipment available in the laboratories. Combined with the gel phase of the system existing at low temperatures and the requirement of the sample of not being exposed to open air to keep the solvent for evaporating, a decision was made to change the approach to analyze the visual change the system experiences during the phase transition.

5.2.3. Visual identification

Using a 10 mL sample for the first iteration of the visual identification experiment proved to be impractical due to the difficulty of observing the transition happening around the thermometer probe in a sample with that amount of material. However, this was a step in the right direction, it showed that the visual characteristic of the phase transition showed promise to be used to predict the transition temperature.

The following step taken was the reduction from a 10 mL sample in a glass vial to a 1.5 mL sample inside an Eppendorf tube. This change allowed for a better visualization of the phase transition process due to the smaller size of the sample, increasing the user-friendliness of the method. In spite of this, the results still lacked the desired repeatability, as shown in the following table.

Table 5.4. *Eppendorf tube transition temperature experiment results.*

Sample	T. Temp (°c)
1	-3,7
2	4,5
3	-0,2
4	3,1
5	5,6
6	-1,1

The results obtained from this experimental set-up are found in table 5.4 and it is observable how the data still suffers from a high variability. This was attributed to the difficulty of securing the thermometer probe inside the sample in a way it would not touch one of the edges or move once the phase transition started. Additionally, the small size of the Eppendorf tubes proved to be difficult to handle in a rudimentary set-up as the one being used for this experiment. Consequently, a more convenient vessel was arranged to contain the PCL sample.

Hence, the third iteration of the visual identification experiment used long and thin micropipettes of 5 mL and 1 mL. By doing this, the quality of the results improved significantly and allowed for deeper studies of the behavior of the system. The fourth iteration including the acrylic vials happened shortly after. Thus, the testing to understand the viability of these new containers.

Table 5.5. *5 mL, 2 mL and acrylic vial transition temperature experiment results.*

	Transition temperature (°C)		
Sample	**5mL pipet (BP)**	**2mL pipet (SP)**	**Acrylic vial (V)**
1	8,2	8,8	8,7
2	8,9	8,8	8,5
3	7,9	8,1	9,0
4	8,7	8,6	8,4
5	8,2	8,1	8,0
6	8,4	7,9	8,5

Table 5.5 shows the first satisfactory results obtained from this experimental path. The three different vessels were evaluated and gave similar and repeatable results. Indicating that the experiments progressed in the right direction. In spite of all three containers working correctly for the measurement, the decision of only using the 5 mL micropipette and the acrylic vial for further measurements was made. The reason being that the 2 mL micropipette offered similar results as its 5 mL, with a more tedious set-up. Due to its smaller diameter, the insertion of the thermometer probe was more challenging.

Finally, the selected preferred container for the sample measurement in the end was the acrylic vial. This is because of its easier to operate geometry and the translucency of its walls. The 5 mL pipet was still used to have a comparison in the further phase transition experimental designs carried out with the visual identification method. As an additional note, during the visual identification experiments a pattern became apparent. Some samples showed a noticeable slowing down in the temperature increase around the phase transition temperature. Thus, inspiration was acquired to find a way to record the temperature profile in order to understand if this thermal “plateau” was observable and measurable.

5.2.4. Laser-Thermometer set-up

As mentioned in the previous chapter, once the acrylic vial was declared as a reliable container for the phase transition study, the next logical step was to replace the human observer with a mechanism capable of recording quantitative data to back up the claims of the reliability of the experimental set-up. The laser-photodiode combination proved to be capable of replacing the human eye; furthermore, with the addition of the LabVIEW software new quantitative photo-data appeared as proof of the phase transition. Additionally, the recording of temperature profiles was made possible by incorporating the VeePro software and connecting it to the thermometer in order to record its data output. The data from both softwares is exported and plotted in excel, resulting in the following type of graphs.

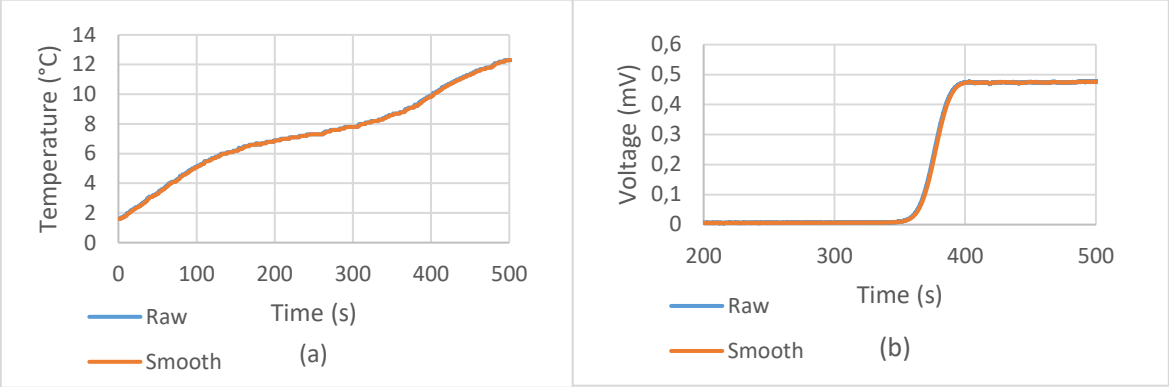

Fig 5.3. (a) *Temperature profile and* ***(b)*** *photodiode data for a sample of 8% PCL in solvent system 1:1:1.*

The two graphs shown in figure 5.3 contain the raw data measured directly in the experiment and an additional set of data that is calculated by applying exponential smoothing to the raw data. The objective being reducing as much as possible the noise and variability present in the laboratory equipment used for the measurement. Exponential smoothing is done by applying the following equation [42].

$$y_0 = x_0 \quad ; \quad y_t = \alpha x_{t-1} + (1-\alpha) y_{t-1} \qquad (5.1)$$

Where the smoothing factor (α) is 0.9 and t represents the time. In figure 5.3 the change is unperceivable, the reason being the great quantity of data, in the data sheet it is possible to observe the step-like increments obtained from the thermometer and the oscillatory signal obtained from the photodiode. Given this situation, the smoothing of the data was required in order for it to be useable in the future analysis.

Data coming from this experimental set-up was reliable and did not show variability. After repeating the experiments, the profiles coming from the thermometer and the photodiode were both regarded as consistent. A major outcome is the confirmation of the thermal plateau in the temperature profile of most of the analyzed samples. This plateau indicates the presence of a latent heat, evidence of a phase transition taking place. However, the plateau is not observable in every sample, which can be explained by a subject mentioned in the state-of-the-art chapter. Thermoreversible gels can have up to three different mechanisms acting

in the creation of the 3D network that is responsible for generating the transition from solution to gel once the sample is cooled down. Depending on a variety of variables from the system and the conditions at which the gel is formed, the three mechanisms will have a different share of the participation on the formation of the gel. If one of the mechanisms does not generate a latent heat during the phase transition and this mechanism is the main participant in the formation of the gel for that sample, then the thermal plateau will be almost undistinguishable in the temperature profile. Thus, different samples show different temperature profiles due to the gel forming mechanisms having a different degree of participation for each case.

On the other hand, the photodiode data shows the same behavior for all the studied samples. There was one emerging issue which was not completely addressed but identified. Due to the fact that the thermometer probe and the laser-photodiode cannot collect data from the same exact region of the sample (the thermometer probe can block the laser signal from reaching the photodiode), there is a synchronization problem between the data collected by these two sensors. The error is slightly amplified by the fact that it was not possible to connect both sensors to the same software; thus, the data collected in each software was started manually as close as possible, with the possibility of human error being present. This was partially subverted by designing caps for the acrylic vials capable of holding the thermometer probe in place as close as possible to the region where the laser-photodiode collect its data. However, the desynchronization issue was not completely resolved in this project.

The method used to find the specific value of the transition temperature is by obtaining the second derivative from these profiles, derivation done based on time. In the case of the temperature profile, the first and second derivative can show the specific point at which the temperature change is the slowest, indicating the moment when the system is using energy to break the additional bonds formed in the gel phase. The following graph shows an example of how these derivatives look, as well as their smoothed version, using eq. 5.1.

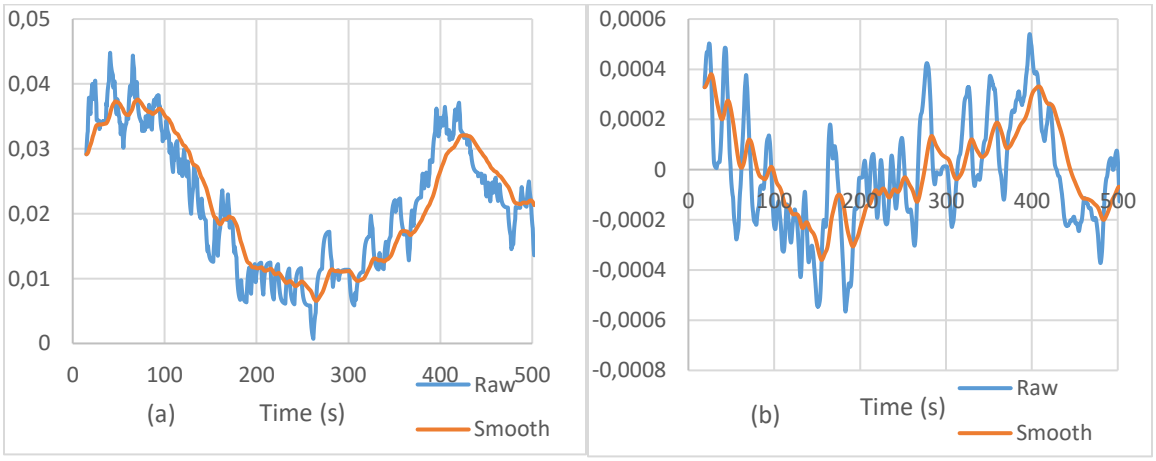

Fig 5.4. (a) *First and* ***(b)*** *second derivative of the temperature profile of an 8% PCL sample.*

The first derivative shown in figure 5.4(a) has an observable minimum value that corresponds to the same value where the function crosses the x-axis in the plot shown in figure 5.4(b). By

finding the temperature value that matches the time of interest, the transition temperature for the sample is estimated. A similar process is carried out to analyze the data obtained from the photodiode.

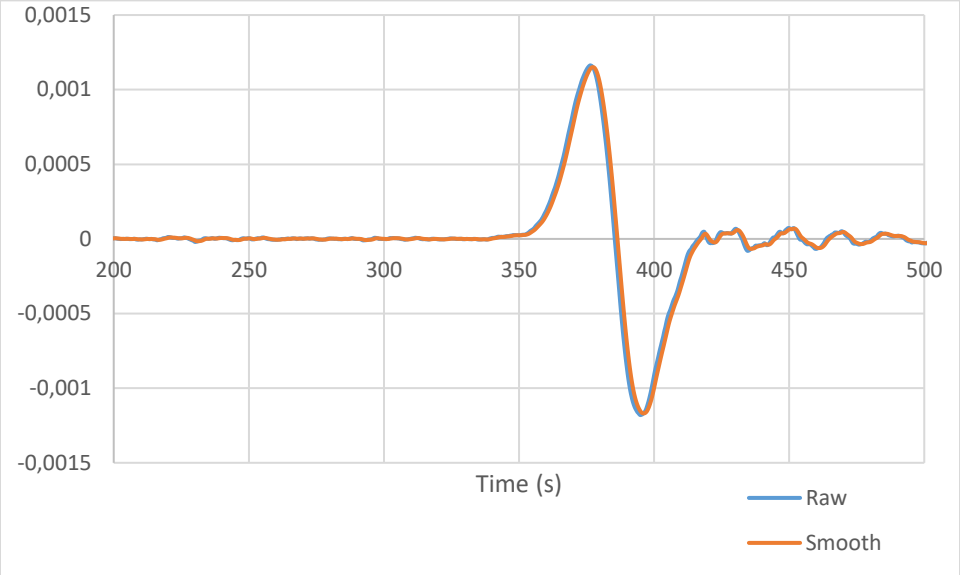

Fig 5.5. *Second derivative of photodiode data profile from an 8% PCL sample.*

In figure 5.5 the second derivative of the photodiode output data in terms of time is presented. The value of interest is located on the maximum peak of the plot. This value represents the time in which the signal received by the photodiode is increasing at the fastest rate. Which in turn indicates the moment when the sample is losing opacity at the fastest rate, in other words, the phase transition is at its peak. Unfortunately, the synchronization issue discussed previously meant that these values are not the same in both graphs. Nonetheless, this is the first iteration of this experimental set-up, which means that there is the possibility of correcting this issue in future work and taking advantage of the potential that this method poses in order to more deeply understand the phase transitions of systems with similar properties to the one being studied in this diploma project.

5.3. PCL/Acetone concentration effect on the transition temperature

Following the experiment designed in subchapter 4.3, the samples were prepared and the experimental set-ups were tested in different occasions. The first experimental trial was done with the third iteration of the visual identification method, using the 5 mL and 1 mL micropipettes, denoted as big and small pipet in the practice. The second trial used the fourth iteration, in other words, the translucent acrylic vials. Finally, the laser method was used for two different repetitions with the same and concentrations but different samples. For the first two trials the temperatures were obtained directly from observation of the sample, whereas the transition temperatures from the third trial were estimated by using the data treatment explained in the previous subchapter (5.2.4). The process used on the data to obtain the

transition temperature for each sample is not shown in this section in favor of brevity and conciseness.

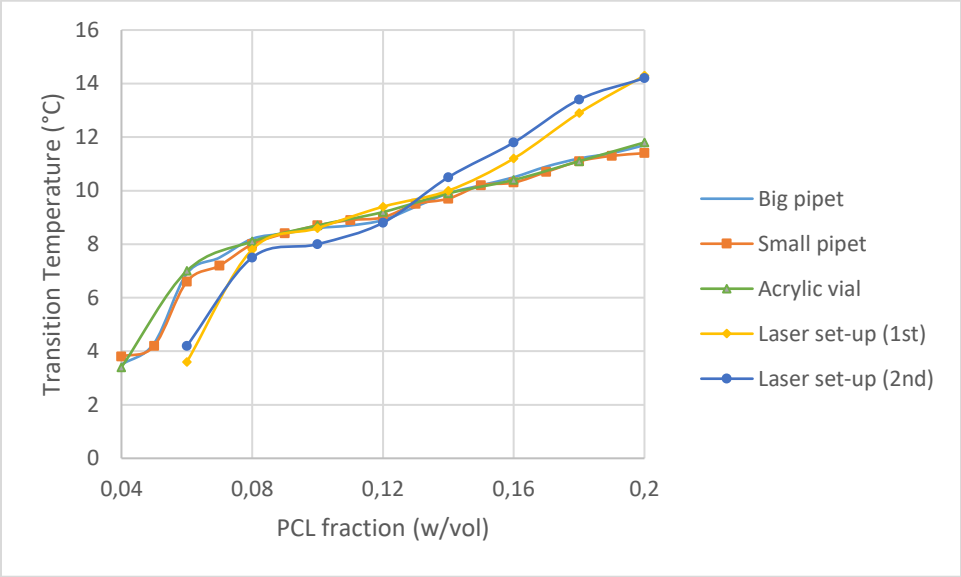

Fig 5.6. *Effect of PCL concentration on transition temperature with a solvent system 1:1:1 as measured by different experimental set-ups.*

The results of these series of experiments are shown in figure 5.6. The first thing that catches the eye is the similarity between the measurements. This is an encouraging sign, confirming that the less reliable third and fourth iterations were not so deviated from the real behavior of the system. Additionally, this validates the idea that combining the laser with the photodiode, a sensor capable of imitating the human eye is obtained to carry out objective visual measurements. In terms of the objective of the experiments, the results show that higher concentrations of PCL in the system lead to higher transition temperatures. This is the expected behavior as increasing the concentration of the polymer gives the gel additional material to create 3D structures; thus, increasing the stability of the gel phase.

Unfortunately, it was not possible to study higher concentrations of PCL due to the saturation of the solvent system and the dissolution process becoming increasing in complexity with the inclusion of additional polymer. Another reason against the deeper exploration of creating PCL solutions of high concentrations is the considerable cost of the PCL. It is a polymer of high cost and it is to be used sparingly in research to avoid the waste of such a valuable resource.

The last experiment carried out in this diploma project is done to evaluate the effect acetone concentration has on the system. This information is relevant for two different reasons. On one hand, the inclusion of acetone in the solvent system gave way to the formation of the gel phase which in turn allowed for the storage of the solution. On the other hand, acetone is a

hazardous solvent as the vapor that comes out of the solvent is flammable and can ignite machinery with moving parts. Therefore, this compound is of significant importance for the system, even if there is a desire to reduce its presence to the minimum due to its hazardous nature.

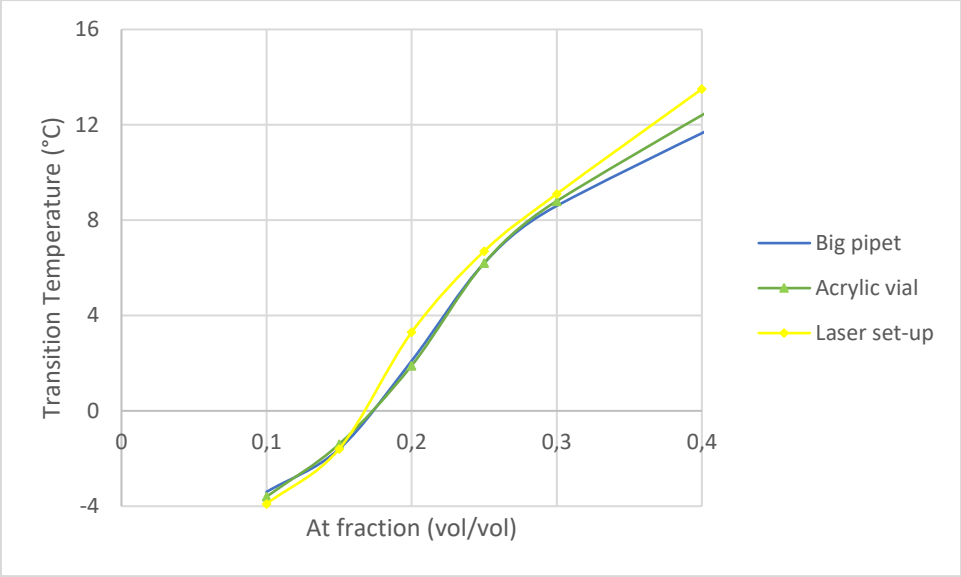

Fig 5.7. *Effect of At concentration on transition temperature with 10% PCL in solvent system 1:1 measured by different methods.*

Figure 5.7 displays the results of the At concentration effect on the transition temperature of the system. It is apparent that the three methods used in the measurements show a similar tendency. The increase of acetone in the system increases significantly the phase transition temperature. This is the expected result, as discussed before, the presence of acetone in the system is what first allowed the formation of the gel phase. Meaning that the acetone molecules generate interactions among the polymeric chains and the other solvent molecules that push the system to form 3D structures when it is cooled down. The desired effect is to increase the stability of the system, as well as decreasing the amount of acetone in order to decrease the flammability factor this solvent brings to the table. As a result, a balance has to be found between these two adverse effects the presence of acetone has in the system.

Both figure 5.6 and figure 5.7 show satisfactory results that allow for the efficient analysis of the collected data and a better understanding of the current state of the system and the possible steps to be taken in the follow-up studies. These data sets are then compared with the mathematical model proposed in the second chapter using the software Wolfram Mathematica.

The first model to be compared with the experimental data is the one proposed in equation (2.20).

$$T = \frac{z\Delta\varepsilon}{k_B}\left[\frac{2Nc\phi_p(1-\phi_p)}{c(1-\phi_p)+N\phi_p}\right]$$

Obtaining the following plot from Wolfram Mathematica.

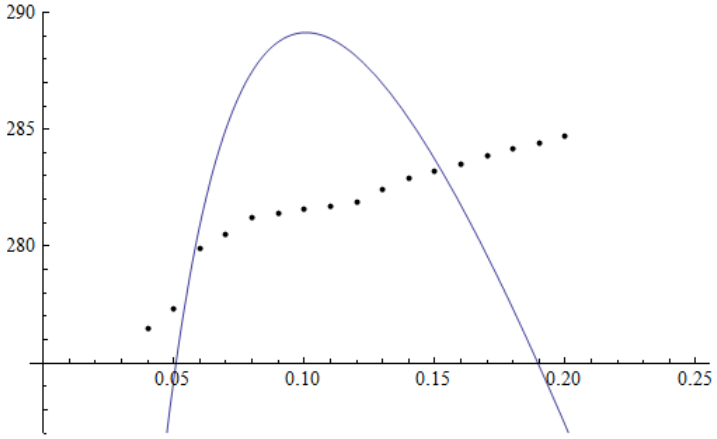

Fig 5.8. *Fitted plot of transition temperature against polymer concentration where the dotted line is the experimental data and the continuous line represents the mathematical model prediction (equation 2.20)*

As it is evident in figure 5.8, the mathematical model from equation (2.20) does not present a good fit when compared to the experimental data. Thus, confirming that this basic mathematical model is not robust enough to correctly predict the behavior of a complex multi-solvent system like the one being analyzed on this diploma project. The additional change in internal energy of this kind of system is not covered in a satisfactory way by this basic model, as mentioned before, there are additional gel forming mechanisms that are generating entropic energy that is unaccounted for in this mathematical model. Therefore, equation (2.22) is expected to perform better.

$$T = \frac{z\Delta\varepsilon}{k_B}\left[\frac{2Nc\phi_p(1-\phi_p)}{c(1-\phi_p)+N\phi_p+2GN\phi_p c(1-\phi_p)}\right]$$

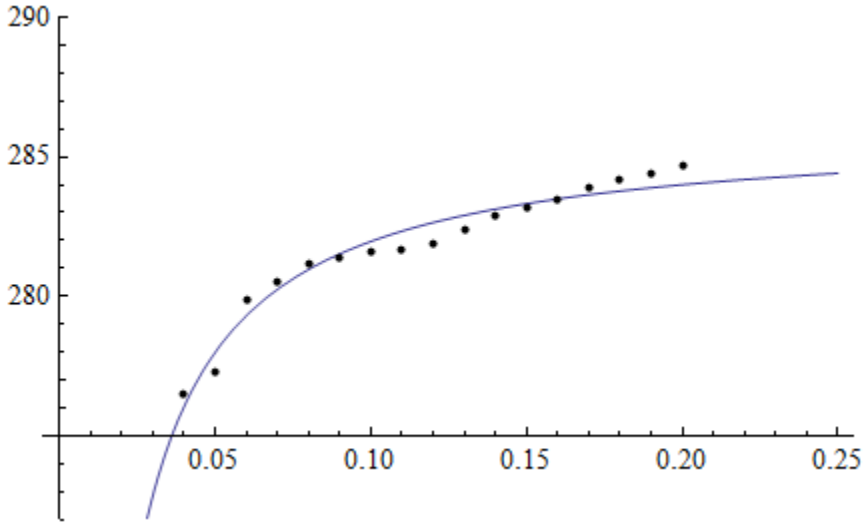

Fig 5.9. *Fitted plot of transition temperature against polymer concentration where the dotted line is the experimental data and the continuous line represents the mathematical model prediction (equation 2.22)*

Figure 5.9 shows a far better fitted curve with values of N=23645, c=91 and G=3.8. The value for N is of the expected order of magnitude for a polymer chain, in the case of c the value is higher than expected for the average size for the solvent clusters (expected to be around 20); nonetheless, it is an acceptable value which can be perfected with the polishing of the mathematical model and the experimental methods. Finally, the value of G was expected to be under 1 but as stated previously, it is a good starting point and can be improved with the refinement of the method. This means that equation (2.22) is far better equipped for the understanding and study of the behavior of complex polymer solvent systems such as PCL in AA:FA:At. The additional entropic term ($G\phi_p^2$) is able to bring some kind of representation for the energy introduced by the hydrogen bond association between polymeric chains and possibly solvent clusters, as well as the energy involved with the formation and destruction of polymer crystals through the sol-gel phase transition.

6. CONCLUSION

In this diploma project, an extensive literature review was carried out regarding the present and future of sutures. As well as the importance of their development for the field of medical textiles, as it is the most widely used product for the closure of wounds. The current classification of sutures was explored and it was discussed that this classification is becoming outdated due to the new and complex structures found in modified composite sutures, such as the PCL nanofiber coated suture with a PLA core yarn mentioned in this project. A wide variety of recent articles was found discussing the utility of functionalizing sutures with surface modifications such as plasma treatment, nanoparticle dispersions and nanofiber coatings, among others. The principle of electrospinning was defined and both of its variations were compared due to the relevance the AC version presented for the polymer-solvent system studied in this project.

With a high regard for the current potential PCL has as a material in the field of medical textiles, a concise and brief description of this polymer and its more appealing applications in the area of suture functionalization was compiled. Which make it a desired material due to its valuable biocompatibility and biodegradability properties. To better understand the world of sol-gel systems, a deep consultation was made regarding the different definition of gels and their diverse categorization. The result of this compilation of literature ended up with the definition of the system of interest as a thermoreversible gel, due to its capability of transitioning freely between its gel and solution phases just by being exposed to a change in temperature. Additionally, three different gel forming mechanisms were identified and defined as hydrogen bond association, crystallite formation and liquid-liquid phase separation by spinodal decomposition. This led to the hypothesis that all three gel forming mechanisms are acting at the same time and with different degrees of participation during the sol-gel phase transition.

It was established that the origin of the idea for this project came to be from a related project carried out in TUL, using PCL nanofibers to coat PLA cores. The addition of acetone to the original PCL, AA and FA solution and further refrigeration of the sample gave way to the intrigue for understanding and studying the newly formed sol-gel system. This highlights the importance of creativity, out of the box thinking and resourcefulness as important philosophical cornerstones to keep in mind when carrying out scientific research.

Various experimental set-ups were designed or adapted from the literature with the objective of testing the sol-gel phase transition from a rheological point of view. First, the inverted tube experiment showed promise regarding the possibility of studying the onset of flow in the system as a phase transition indicator. Followed by the micropipette and the U-shaped tube experimental set-ups. Both of these iterations yielded results that indicated that the onset of flow is better studied when deeper knowledge of the system properties is known and a higher control of the variables surrounding the experiment is achieved. The following set of experiments that focused on the visual changes of the system as an indicator of the phase transition yielded more satisfactory results. The initial glass vial and Eppendorf tube set-ups showed potential in the identification of the phase transition but failed in the reliability aspect

due mainly to the size and geometry of the container. On the other hand, the latter 5 mL and 1 mL micropipette visual experiments performed well both in identification viability and repeatability of the results, but was still lacking a way of quantifying the visual aspect of the transition. The culmination of the experimental set-ups came in the form of an apparatus composed of a laser and a photodiode acting as the observer and the thermometer recording the temperature profile of the phase transition. Combining this set-up with specialized software allowed for the recollection of both visual and thermal data of the complete phase transition of different samples.

A simplified lattice model based on the Flory-Huggins equation for the free energy of the system was used and expanded in order to better predict the behavior of the samples. Since the standard form of the mathematical model, i.e. spinodal decomposition, found in the literature was too simplistic to define this system, an additional term was suggested and added in order to bring some additional, but limited realism to the equation regarding the existence of hydrogen bond association and crystallite formation as gel forming mechanisms parallel to spinodal decomposition. The comparison of both of these models with the experimental data yielded the expected results, leading to the conclusion that highly complex systems like the one studied in this project are not easily describable by simpler models that exclude additional internal processes happening alongside the main processes.

Finally, it would be interesting to dive deeper into the effect acetone has on the system by studying in more detail the interactions this compound has with the other solvents and similar systems. Furthermore, for future work with the laser set-up it is recommended to explore the use of different kinds of thermal probes in order to improve the synchronization issues between photo-signal and the thermal signal, as well as improving the reading of the thermal plateau present around the phase transition temperature. On the other hand, future research on the gelation mechanisms present in the sol-gel transition could help shed some light on this puzzling matter and bring forth new ideas to implement standardized measurements appliable to a wider arrange of thermoreversible gels.

7. REFERENCES

[1] W. Cao and R. M. Cloud, “14 - Balancing comfort and function in textiles worn by medical personnel,” in *Woodhead Publishing Series in Textiles*, G. B. T.-I. C. in C. Song, Ed. Woodhead Publishing, 2011, pp. 370–384.

[2] S. Akter, A. Y. M. Azim, and M. A. Al Faruque, “MEDICAL TEXTILES: SIGNIFICANCE AND FUTURE PROSPECT IN BANGLADESH,” vol. 1010, pp. 1857–7881, May 2014.

[3] Y. R. Park *et al.*, “Three-dimensional electrospun silk-fibroin nanofiber for skin tissue engineering,” *Int. J. Biol. Macromol.*, vol. 93, pp. 1567–1574, Dec. 2016.

[4] N. Gokarneshan and K. Velumani, “Recent Innovations in Textile Sutures - An Approach towards Improved Surgical Procedures,” *Sci. c J. Biomed. Eng. Biomed. Sci.*, vol. 2, no. 1, pp. 001–007, 2018.

[5] C. G. Pitt, F. I. Chasalow, Y. M. Hibionada, D. M. Klimas, and A. Schindler, “Aliphatic polyesters. I. The degradation of poly(ϵ-caprolactone) in vivo,” *J. Appl. Polym. Sci.*, vol. 26, no. 11, pp. 3779–3787, Nov. 1981.

[6] I. Adekogbe and A. Ghanem, “Fabrication and characterization of DTBP-crosslinked chitosan scaffolds for skin tissue engineering,” *Biomaterials*, vol. 26, no. 35, pp. 7241–7250, 2005.

[7] M. King, “Overview of opportunities in medical textiles,” *Can. Text. J.*, vol. 118, pp. 34–36, Jan. 2001.

[8] C. C. Chu, J. A. von Fraunhofer, and H. P. Greisler, *Wound Closure Biomaterials and Devices*. Taylor & Francis, 1996.

[9] D. Kojić *et al.*, *STRUCTURING OF POLYMER MATERIALS FOR ABSORBABLE SURGICAL SUTURES*. 2017.

[10] M. Aslan, M. Bykkurt, and Yildirim, “Comparison of different absorbable suture materials in skin closure: An experimental study in rats,” *Pain Clin.*, vol. 17, pp. 81–88, Mar. 2005.

[11] A. R. Horrocks and S. C. Anand, *Handbook of technical textiles*. 2000.

[12] I.-H. Loh, H.-L. Lin, and C. C. Chu, “Plasma surface modification of synthetic absorbable sutures,” *J. Appl. Biomater.*, vol. 3, no. 2, pp. 131–146, Jun. 1992.

[13] J. Pionteck and G. B. T.-H. of A. (Second E. Wypych, Eds., “10 - ANTISTATIC AGENT INCORPORATION METHOD AND ITS PERFORMANCE,” ChemTec Publishing, 2016, pp. 129–139.

[14] M. Sivan *et al.*, “Plasma treatment effects on bulk properties of polycaprolactone nanofibrous mats fabricated by uncommon AC electrospinning: A comparative study,” *Surf. Coatings Technol.*, vol. 399, p. 126203, 2020.

[15] A. Visco, C. Scolaro, A. Giamporcaro, S. De Caro, E. Tranquillo, and M. Catauro, "Threads Made with Blended Biopolymers: Mechanical, Physical and Biological Features," *Polymers (Basel).*, vol. 11, no. 5, p. 901, May 2019.

[16] E. J. Lee *et al.*, "Application of Materials as Medical Devices with Localized Drug Delivery Capabilities for Enhanced Wound Repair," *Prog. Mater. Sci.*, vol. 89, pp. 392–410, Aug. 2017.

[17] C. C. Chu, "10 - Types and properties of surgical sutures," in *Woodhead Publishing Series in Textiles*, M. W. King, B. S. Gupta, and R. B. T.-B. as M. I. Guidoin, Eds. Woodhead Publishing, 2013, pp. 231–273.

[18] A. Arora, G. Aggarwal, J. Chander, P. Maman, and M. Nagpal, "Drug eluting sutures: A recent update," *J. Appl. Pharm. Sci.*, vol. 9, no. 07, pp. 111–123, 2019.

[19] R. Abhari, A. Carr, and P.-A. Mouthuy, "Multifilament electrospun scaffolds for soft tissue reconstruction," in *Electrofluidodynamic Technologies (EFDTs) for Biomaterials and Medical Devices: Principles and Advances*, 2018, pp. 295–328.

[20] S. Chen *et al.*, "Nanofiber-based sutures induce endogenous antimicrobial peptide," *Nanomedicine*, vol. 12, no. 21, pp. 2597–2609, Sep. 2017.

[21] Y.-Z. Long, X. Yan, X.-X. Wang, J. Zhang, and M. Yu, "Chapter 2 - Electrospinning: The Setup and Procedure," in *Micro and Nano Technologies*, B. Ding, X. Wang, and J. B. T.-E. N. and A. Yu, Eds. William Andrew Publishing, 2019, pp. 21–52.

[22] V. Kumar, S. Naqvi, and P. Gopinath, "Application[1] V. Kumar, S. Naqvi, and P. Gopinath, 'Applications of Nanofibers in Tissue Engineering,' Appl. Nanomater., pp. 179–203, Jan. 2018.s of Nanofibers in Tissue Engineering," *Appl. Nanomater.*, pp. 179–203, Jan. 2018.

[23] G. Yan, H. Niu, and T. Lin, "Chapter 7 - Needle-less Electrospinning," in *Micro and Nano Technologies*, B. Ding, X. Wang, and J. B. T.-E. N. and A. Yu, Eds. William Andrew Publishing, 2019, pp. 219–247.

[24] D. Lukas *et al.*, "Effective AC needleless and collectorless electrospinning for yarn production," *Phys. Chem. Chem. Phys.*, vol. 16, Oct. 2014.

[25] L. McKeen, "12 - Renewable Resource and Biodegradable Polymers," in *Plastics Design Library*, L. B. T.-T. E. of S. on P. and E. (Third E. McKeen, Ed. Boston: William Andrew Publishing, 2012, pp. 305–317.

[26] L. S. Nair and C. T. Laurencin, "Biodegradable polymers as biomaterials," *Prog. Polym. Sci.*, vol. 32, no. 8, pp. 762–798, 2007.

[27] F. Tanaka, "Polymer Physics: Applications to Molecular Association and Thermoreversible Gelation," *Polym. Phys. Appl. to Mol. Assoc. Thermoreversible Gelation*, pp. 1–387, 2011.

[28] "Definitions of terms relating to the structure and processing of sols, gels, networks, and inorganic-organic hybrid materials (IUPAC Recommendations 2007) ," *Pure and Applied Chemistry* , vol. 79. p. 1801, 2007.

[29] S. E. Friberg, "Interactions of Surfactants with Polymers and Proteins. E.D.Goddard and K.P. Ananthapadmanabhan (eds.), CRC Press, Boca Raton, FL, 1993, pp. 1-427, $169.95," *J. Dispers. Sci. Technol.*, vol. 15, no. 3, p. 399, Jan. 1994.

[30] K. Kawanishi, M. Komatsu, and T. Inoue, "Thermodynamic consideration of the sol-gel transition in polymer solutions," *Polymer (Guildf).*, vol. 28, no. 6, pp. 980–984, 1987.

[31] L. Mandelkern, "11 - Crystallization and Melting," G. Allen and J. C. B. T.-C. P. S. and S. Bevington, Eds. Amsterdam: Pergamon, 1989, pp. 363–414.

[32] E. Pines and W. Prins, "Structure-Property Relations of Thermoreversible Macromolecular Hydrogels," *Macromolecules*, vol. 6, no. 6, pp. 888–895, Nov. 1973.

[33] S. R. Raghavan and B. H. Cipriano, "Gel Formation: Phase Diagrams Using Tabletop Rheology and Calorimetry BT - Molecular Gels: Materials with Self-Assembled Fibrillar Networks," R. G. Weiss and P. Terech, Eds. Dordrecht: Springer Netherlands, 2006, pp. 241–252.

[34] M. A. Harrison, P. H. Morgan, and G. S. Park, "A simple method for determining sol—gel transition temperatures in weak polymer jellies," *Br. Polym. J.*, vol. 3, no. 3, pp. 154–155, May 1971.

[35] D. Lukas, N. Asatiani, V. Jencova, E. Kostakova, and P. Mikes, *Fyzika polymeru*, 2nd ed. Liberec: Technical University of Liberec, 2018.

[36] D. Hestenes, "Entropy and Indistinguishability," *Am. J. Phys.*, vol. 38, no. 7, pp. 840–845, Jul. 1970.

[37] D. Jadhav, N. K. Karthick, P. P. Kannan, S. Ramasamy, A. Elangovan, and G. Arivazhagan, "Molecular interaction forces in acetone + ethanol binary liquid solutions: FTIR and theoretical studies," *J. Mol. Struct.*, vol. 1130, p. 497, Oct. 2016.

[38] Y. Ohya, S. Maruhashi, T. Hirano, and T. Ouchi, "Preparation of Poly(lactic Acid)-Grafted Polysaccharides as Biodegradable Amphiphilic Materials BT - Biomedical Polymers and Polymer Therapeutics," E. Chiellini, J. Sunamoto, C. Migliaresi, R. M. Ottenbrite, and D. Cohn, Eds. Boston, MA: Springer US, 2002, pp. 139–148.

[39] N. Lavielle *et al.*, "Controlled formation of poly(ε-caprolactone) ultrathin electrospun nanofibers in a hydrolytic degradation-assisted process," *Eur. Polym. J.*, vol. 49, no. 6, pp. 1331–1336, 2013.

[40] L. A. Bosworth and S. Downes, "Acetone, a Sustainable Solvent for Electrospinning Poly(ε-Caprolactone) Fibres: Effect of Varying Parameters and Solution Concentrations on Fibre Diameter," *J. Polym. Environ.*, vol. 20, no. 3, pp. 879–886, 2012.

[41] Y. Masubuchi and T. Uneyama, “Retardation of the reaction kinetics of polymers due to entanglement in the post-gel stage in multi-chain slip-spring simulations,” *Soft Matter*, vol. 15, no. 25, pp. 5109–5115, 2019.

[42] NIST/SEMATECH, “e-Handbook of Statistical Methods,” 2003. [Online]. Available: https://www.itl.nist.gov/div898/handbook/. [Accessed: 02-Jan-2021].